

1 **Beyond the reference: gene expression variation and transcriptional response to RNAi in**
2 ***C. elegans***

3
4 Avery Davis Bell*, Han Ting Chou, Annalise B. Paaby*
5 School of Biological Sciences, Georgia Institute of Technology, Atlanta, GA

6 *Correspondence: averydavisbell@gmail.com; paaby@gatech.edu
7

8 **Abstract**

9 A universal feature of living systems is that natural variation in genotype underpins variation in
10 phenotype. Yet, research in model organisms is often constrained to a single genetic
11 background, the reference strain. Further, genomic studies that do evaluate wild strains typically
12 rely on the reference strain genome for read alignment, leading to the possibility of biased
13 inferences based on incomplete or inaccurate mapping; the extent of reference bias can be
14 difficult to quantify. As an intermediary between genome and organismal traits, gene expression
15 is well positioned to describe natural variability across genotypes generally and in the context of
16 environmental responses, which can represent complex adaptive phenotypes. *C. elegans* sits at
17 the forefront of investigation into small-RNA gene regulatory mechanisms, or RNA interference
18 (RNAi), and wild strains exhibit natural variation in RNAi competency following environmental
19 triggers. Here, we examine how genetic differences among five wild strains affect the *C.*
20 *elegans* transcriptome in general and after inducing RNAi responses to two germline target
21 genes. Approximately 34% of genes were differentially expressed across strains; 411 genes
22 were not expressed at all in at least one strain despite robust expression in others, including 49
23 genes not expressed in reference strain N2. Despite the presence of hyper-diverse hotspots
24 throughout the *C. elegans* genome, reference mapping bias was of limited concern: over 92% of
25 variably expressed genes were robust to mapping issues. Overall, the transcriptional response
26 to RNAi was strongly strain-specific and highly specific to the target gene, and the laboratory
27 strain N2 was not representative of the other strains. Moreover, the transcriptional response to
28 RNAi was not correlated with RNAi phenotypic penetrance; the two germline RNAi incompetent
29 strains exhibited substantial differential gene expression following RNAi treatment, indicating an
30 RNAi response despite failure to reduce expression of the target gene. We conclude that gene
31 expression, both generally and in response to RNAi, differs across *C. elegans* strains such that
32 choice of strain may meaningfully influence scientific conclusions. To provide a public, easily
33 accessible resource for querying gene expression variation in this dataset, we introduce an
34 interactive website at <https://wildworm.biosci.gatech.edu/rnai/>.

35 Introduction

36 Research in the model organism *C. elegans* has yielded insight into myriad aspects of biology,
37 particularly development, genetics, and molecular biology (Corsi et al., 2015). Historically, much
38 of this work has been conducted in a single isogenic strain, the laboratory strain N2 (Andersen
39 et al., 2012; Antoine Barriere & M. A. Felix, 2005). However, *C. elegans* harbors significant
40 intraspecific genetic diversity (A. Barriere & M. A. Felix, 2005; Antoine Barriere & M. A. Felix,
41 2005; Crombie et al., 2019; Lee et al., 2021; Andersen et al., 2012), and in the last decade *C.*
42 *elegans* has also been established as a powerful system for elucidating connections between
43 genotype and phenotype (Andersen et al., 2012; Andersen & Rockman, 2022; A. Barriere & M.
44 A. Felix, 2005; Antoine Barriere & M. A. Felix, 2005; Cook et al., 2017; Crombie et al., 2019;
45 Evans, van Wijk, et al., 2021; Gaertner & Phillips, 2010; Lee et al., 2021). Natural genetic
46 variation exists for practically any organismal trait measurable in *C. elegans* (Andersen &
47 Rockman, 2022), for example: responsiveness to toxins, metals, drugs, and other stressors
48 (Dilks et al., 2021; Evans & Andersen, 2020; Evans, Wit, et al., 2021; Hahnel et al., 2018; Na et
49 al., 2020; Webster et al., 2019; Zdraljevic et al., 2019; Zdraljevic et al., 2017); behavior
50 (Bendesky et al., 2012; Ghosh et al., 2015; McGrath et al., 2009); transgenerational mortality
51 traits (Frezal et al., 2018; Saber et al., 2022); and efficiency in RNA interference (RNAi) (Elvin et
52 al., 2011; Felix, 2008; Felix et al., 2011; Paaby et al., 2015; Tijsterman et al., 2002).

53

54 Naturally, molecular phenotypes that act as intermediaries between genotype and organismal
55 traits, such as gene expression, also vary across strains. Studies from recombinant inbred lines
56 (Evans & Andersen, 2020; Rockman et al., 2010; Vinuela et al., 2010) and, more recently, RNA
57 sequencing of 207 wild strains (Zhang et al., 2022), have identified numerous expression
58 quantitative trait loci (eQTL) that encode differences in gene expression. How such expression
59 differences manifest across different strains, whether they offer clues into functional
60 differentiation, and how genetic differences compare to environmentally induced differences in
61 gene expression or mediate gene expression responses to environmental stimuli remain
62 interesting questions. These questions require genome-wide characterization of gene
63 expression in multiple strains under multiple conditions.

64

65 One phenomenon of particular interest is RNA interference, a mechanism of gene expression
66 regulation triggered by environmental or endogenous sources of double stranded RNA with
67 broad-reaching influence over diverse aspects of organismal biology (Billi et al., 2014; Wilson &
68 Doudna, 2013). RNAi was discovered in *C. elegans* (Fire et al., 1998), but competency in

69 response to environmental triggers is highly variable across wild *C. elegans* strains (Elvin et al.,
70 2011; Felix, 2008; Felix et al., 2011; Paaby et al., 2015; Tijsterman et al., 2002). Previous work
71 showed that a loss-of-function mutation in Argonaute RNAi effector gene *ppw-1* is largely
72 responsible for the near-complete failure of Hawaiian strain CB4856 to mount an RNAi
73 response against germline targets (Tijsterman et al., 2002), and later work characterized the
74 failure in CB4856 as a much delayed, rather than absent, response (Chou et al., 2022). Other
75 strains incompetent for germline RNAi exhibit distinct modes of RNAi failure with distinct genetic
76 bases (Chou et al., 2022; Elvin et al., 2011; Pollard & Rockman, 2013). Even as wild strains
77 vary in overall competency for germline RNAi, strain-to-strain differences in RNAi phenotypic
78 penetrance are also highly dependent on the target gene; whether these differences arise from
79 strain-specific developmental consequences of gene knock-down or strain-specific differences
80 in target-dependent RNAi efficacy is unclear (Paaby et al., 2015). How this phenotypic variation
81 in RNAi response is reflected in genome-wide transcriptional changes upon RNAi induction
82 remains a largely open question.

83
84 Here, we evaluate how genotype (strain) and induction of the RNAi response affect the *C.*
85 *elegans* transcriptome. We also consider how reliance on the reference genome, derived from
86 the laboratory strain N2, might constrain estimates of gene expression in wild strains, and how a
87 focus on N2 in studies of RNAi might limit inferences about RNAi biology within *C. elegans*
88 generally. To investigate these questions, and to provide a public resource for interrogating
89 transcriptional variation in this system, we performed RNA sequencing on five *C. elegans*
90 strains with varying competency in germline RNAi, both in the control condition and under RNAi
91 treatment targeting two germline-expressed genes.

92

93 **Materials and methods**

94 **Sample preparation and sequencing**

95 *Worm strains and husbandry*

96 Strains used in this study include wild strains CB4856, EG4348, JU1088, and QX1211 (gifts
97 from Matthew Rockman) and wild-type laboratory strain N2 (gift from Patrick McGrath). Worms
98 were cultured under standard conditions (Stiernagle, 2006) except that plates used for non-N2
99 wild strains were made with 1.25% agarose to prevent burrowing. All strains except for QX1211
100 were maintained at 20°C; QX1211 was maintained at 18°C to prevent induction of its mortal
101 germline phenotype (Frezal et al., 2018). Worms were maintained for at least three generations
102 without starvation before RNAi induction and RNA sequencing.

103

104 *RNA interference*

105 RNAi was induced via feeding and was carried out on plates at 20°C following established
106 methods (Ahringer, 2006; Kamath et al., 2001). Worms were fed HT115 *E. coli* bacteria that had
107 been transformed with the empty pL4440 vector or the pL4440-derived vectors *par-1*
108 (H39E23.1) and *pos-1* (F52E1.1) from the Ahringer feeding library (Kamath & Ahringer, 2003).
109 Bacteria cultures were prepared by streaking from frozen stocks onto LB agar with carbenicillin
110 (25 ug/mL) and tetracycline (12.5 mg/mL); next 5-10 colonies from < 1 week old plates were
111 used to inoculate liquid cultures of LB broth with carbenicillin (50 ug/mL) and tetracycline (12.5
112 mg/mL), which were then incubated with shaking at 37°C for 16-18 hours and finally amplified
113 with carbenicillin (50 ug/mL) for 6hrs at a 1:200 dilution. 10cm agar feeding plates with 1mM
114 IPTG (Ahringer 2006) were seeded with the RNAi bacteria cultures, then used within 44-78
115 hours after incubation in the dark. Worm strains reared under standard conditions were
116 bleached on day 1 to synchronize, then bleached again on day 4 (Stiernagle, 2006). On day 5,
117 L1s were transferred to the RNAi plates. All strains were exposed to RNAi in this way at the
118 same time in triplicate, 6 total plates per strain.

119

120 *RNA library preparation and sequencing*

121 As previously described (Chou et al., 2022), synchronized hermaphrodites reared on RNAi
122 feeding plates were washed off at the first sign of egg laying, washed twice with M9 buffer, and
123 stored in TRIzol (Invitrogen #15596026) at -80°C until RNA extraction. RNA was extracted from
124 all samples at the same time using TRIzol (Invitrogen #15596026) and RNeasy columns
125 (Qiagen #74104) following (He, 2011). cDNA and sequencing libraries were generated from 500
126 ng of fresh RNA samples with 10 cycles of PCR with the NEBNext Ultra II Directional RNA
127 Library Prep Kit for Illumina (NEB #7760). After quality checking using an Agilent 2100
128 Bioanalyzer, library fragments were size-selected via BluePippon (Sage Science). Single-end
129 75bp reads were sequenced on an Illumina NextSeq at the Molecular Evolution Core facility at
130 the Georgia Institute of Technology.

131

132 **Analysis**

133 *Analytical approach*

134 We considered multiple state-of-the-art pipelines to align RNA-seq data and quantify
135 expression. Because the four wild strains in our study are diverged from the N2 reference
136 genome by differing degrees (Cook et al., 2017), we required a method that could evaluate N2

137 data and non-N2 data over a range of variation without bias. One variant-aware option for
138 quantifying RNA expression is to consider only RNA-seq reads that align to exactly one position
139 on the reference genome (unique mappers) using STAR (Dobin et al., 2012), and to discard
140 reads not uniquely aligning to the same position after non-reference variants are swapped into
141 the read using WASP (van de Geijn et al., 2015). We explored this approach with our data.
142 Specifically, we used STAR v2.7.5a with non-default parameters `--outFilterMismatchNmax 33 --`
143 `seedSearchStartLmax 33 --alignSJoverhangMin 8 --outFilterScoreMinOverLread 0.3 --`
144 `alignIntronMin 40 --alignIntronMax 2200 --waspOutputMode SAMtag --varVCFfile <VCF`
145 `containing SNPs from all 4 non-reference strains>; these latter parameters implemented WASP`
146 `from within STAR.`

147
148 A second option is to generate strain-specific transcriptomes that incorporate known variants
149 from each strain into the reference genome and use those to quantify transcript expression via
150 pseudo-alignment; this approach permits reads to map to multiple locations (Bray et al., 2016;
151 Patro et al., 2017). We do not compare the STAR-WASP approach to this pseudo-alignment
152 approach here; high-level results were similar between the approaches. For our final analysis
153 we chose the second option, for multiple reasons: 1) pseudo-alignment approaches are at least
154 as accurate at estimating expression while being computationally more efficient (Bray et al.,
155 2016; Patro et al., 2017); 2) pseudo-alignment approaches take into account the large fraction
156 of reads that align to multiple loci in the genome (Bray et al., 2016; Patro et al., 2017); and 3)
157 our specific generation of strain-specific transcriptomes enabled us to include insertion-deletion
158 polymorphisms (INDELs), whereas WASP ignores INDELs (van de Geijn et al., 2015). Including
159 INDELs was particularly relevant in this study, as 8,195-67,267 INDELs differentiate the four
160 non-reference strains from the reference genome (CeNDR 20210121 release) (Cook et al.,
161 2017).

162
163 The following methods detail generation of strain-specific transcriptomes and pseudo-alignment
164 to quantify expression at individual genes. A subset of these methods and data overlap with our
165 recent RNAi-focused study, which examined expression variation at specific RNAi genes (Chou
166 et al., 2022).

167 168 *Strain-specific transcriptomes*

169 As previously described (Chou et al., 2022), we used SNPs and INDELs from CeNDR (release
170 20210121) (Cook et al., 2017) to update the N2 reference genome (release ws276) (Harris et

171 al., 2020) to generate strain-specific transcriptomes using the software *g2gtools* (v0.1.31 via
172 conda v4.7.12, Python v2.7.16) (<https://github.com/churchill-lab/g2gtools>). Specifically, INDELS
173 were added to the reference genome with *g2gtools vcf2chain* and SNPs with *g2gtools patch*.
174 INDELS were added to the SNP-updated genome with *g2gtools transform*. We generated strain-
175 specific GTFs from the strain-specific FASTAs with *g2gtools convert* and generated strain-
176 specific transcriptomes from these GTFs with *gffread* (v0.12.7) (Pertea & Pertea, 2020).

177

178 The nextflow workflow performing this process is available in this project's code repository
179 (<https://github.com/averydavisbell/wormstrainrnaexpr>) in *workflows/strainspectranscriptome*.

180

181 *Gene expression quantification*

182 Transcript-level quantification, used downstream for gene-level estimates, was performed using
183 Salmon (v1.4.0) (Patro et al., 2017), as we previously detailed (Chou et al., 2022). First, we
184 trimmed Illumina TruSeq adapters from RNA-seq reads with Trimmomatic (v0.3.9) (Bolger et al.,
185 2014), parameters *ILLUMINACLIP:TruSeq3- SE.fa:1:30:1*. Strain-specific transcriptomes were
186 used to generate Salmon index files with command *salmon index* with options *-k 31 --*
187 *keepDuplicates* (all others default; no decoy was used). Salmon transcript quantification *salmon*
188 *quant* was performed with options *-l SR --dumpEq, --rangeFactorizationBins 4, --seqBias, and --*
189 *gcBias*, and library-specific fragment length arguments *--fldMean* and *--fldSD*.

190

191 The nextflow workflow generating strain-specific transcriptomes (link above) also generates
192 strain-specific salmon indexes; the nextflow workflow performing transcript quantification is
193 available in this project's code repository in *workflows/strainspeccsalmon*.

194

195 *Differential expression analysis*

196 Differential expression analyses were performed in R (v4.1.0) (R Core Team, 2021) using the
197 DESeq2 package (v1.32.0) (Love et al., 2014). We imported transcript quantification data into
198 DESeq2 using the tximport package (v1.20.0) (Soneson et al., 2015), which adds Salmon-
199 specific transcript length normalizations to DESeq2's sample-wise RNA quantification
200 normalization and converts Salmon's transcriptome quantification estimates to gene-level
201 quantification estimates. Genes with fewer than 10 estimated reads across all samples
202 (summed) were excluded from downstream analyses, retaining 18,589 genes. Principal
203 components analysis was performed using the top 500 most variably expressed genes across

204 all samples after DESeq2's variance-stabilizing transformation (*vst* function), which was
205 performed blind to experimental design.

206

207 We used DESeq2's likelihood-ratio tests to determine whether genes were differentially
208 expressed based on strain in the control condition and whether the interaction of strain and
209 treatment was significant. For strain-wise significance, control sample counts were modeled with
210 the negative binomial model

$$211 \quad \log_2(q_{ij}) = \beta_i x_j + 1$$

212 Which was compared to the reduced (null) model

$$213 \quad \log_2(q_{ij}) = 1$$

214 Here, for gene i , sample j , q is proportional to the actual concentration of RNA fragments for a
215 gene (derived by DESeq2 from input counts and error modeling. (Love et al., 2014). β_i gives the
216 log2 fold changes for gene i corresponding to strain x . A total of 15,654 genes were sufficiently
217 detected in the control samples to be included in this analysis (the remainder were excluded by
218 DESeq2's p-value correcting methods).

219

220 To evaluate strain:treatment interactions, all sample counts were modeled with the negative
221 binomial model

$$222 \quad \log_2(q_{ij}) = \beta_{1i} x_j + \beta_{2i} y_j + \beta_{3i} x_j y_j$$

223 Which was compared to the reduced model

$$224 \quad \log_2(q_{ij}) = \beta_{1i} x_j + \beta_{2i} y_j$$

225 Here, the symbols are as in the first set of equations, with the additions that y corresponds to
226 RNAi treatment; xy to the strain-treatment interaction; and β_1 to the strain effect, β_2 to the
227 treatment effect, and β_3 to the interaction effect.

228

229 In both likelihood-ratio tests, genome-wide adjusted p-values were determined by DESeq2's
230 multiple testing correction. Genes were considered differentially expressed if this p-value was
231 less than 0.1.

232

233 On the same datasets, we assessed differential expression within strains using DESeq2's
234 Wald's tests of contrasts between treated (*par-1* or *pos-1* RNAi) and control (empty vector)

235 samples. Genes were considered significantly differentially expressed if, after log₂ fold change
236 shrinkage using the ‘ashr’ method from the package ashR (v2.2-47) (Stephens, 2017), their
237 absolute value fold change was greater than 1.5 and genome-wide adjusted p-value (FDR) was
238 less than 0.1.

239

240 The script performing these analyses is available in this project’s code repository at
241 *diffexp_lrt_straintreat_salmon_deseq2.R*.

242

243 *DNA sequence coverage estimation and identification of low-coverage and missing genes*

244 We examined DNA sequence coverage within genes in CeNDR (Cook et al., 2017) BAM files
245 (20210121 release); these files correspond to the same strains as in our study except in the
246 case of EG4348, where CeNDR sequenced genetically identical strain EG4349. We note, of
247 course, that the CeNDR DNA alignments were made directly to the N2 genome; we used the
248 variants discovered therein to build our genotype-specific pseudo-transcriptomes. To get per-
249 gene DNA sequence coverage, we first generated a file containing the non-overlapping, non-
250 duplicated locations of all genes’ RNA generating sequences by determining the locations of all
251 merged exons genome-wide using GTFTools (v0.8.5) (Li, 2018)
252 (<http://www.genemine.org/gtftools.php>). Then, we determined the mean per-base coverage of
253 each of these regions using mosdepth v0.3.2 (Pedersen & Quinlan, 2018) with default options
254 with the exception of setting *--flag 1540*, which excludes unmapped reads, PCR duplicates, and
255 QC failures. Finally, we computed the per-gene coverage as

$$256 \frac{\sum(\text{coverage per merged exon} * \text{length of merged exon})}{\sum \text{length merged exons in gene}}$$

257 To delineate a set of low DNA coverage genes, we median-normalized the coverages within
258 strain and flagged any with < 25% of the median coverage (i.e., median-normalized coverage <
259 0.25) as low coverage. Genes were classified as putatively missing from non-reference strain
260 genomes if they had raw coverage estimates of exactly zero.

261

262 The workflow running this analysis is available in this project’s code repository in
263 *workflows/mosdepthmergedexons*; this workflow performs custom gene-level analysis steps by
264 calling an R script available in this project’s code repository at
265 *exploregencoverage_fromexons.R*. The scripts determining overlap with differentially
266 expressed genes and zero-coverage genes are available in this project’s code repository at
267 *de_dnacov_overlap.R* and *exploregencoverage_fromexons_lowend.R*.

268

269 *'Off' gene analysis*

270 To identify genes putatively unexpressed in one or more strains despite being expressed in
271 others ('off' genes), we first identified all genes differentially expressed between any two strains
272 in the control condition (Wald's test comparing each strain pair, genome-wide adjusted $p < 0.1$).
273 The rationale was that genes significant for differential expression between strain pairs must
274 have meaningful expression in at least one strain; we employed this standard to avoid inclusion
275 of genes that are simply not expressed or expressed at a very low level regardless of strain. We
276 then determined the average variance-stabilizing transformed (DESeq2 function *vst*) expression
277 across all samples from all three treatments within each strain for these genes and identified
278 those with zero mean expression. (These genes, of course, also have zero estimated
279 expression prior to *vst* normalization.) Genes with strain-wise differential expression and zero
280 expression within a strain comprise the 'off' gene set. (This process identified an additional six
281 genes that fell just short of significance in the global analysis for differential expression in the
282 likelihood-ratio test described above.) We then interrogated these genes for overlap with low
283 DNA coverage and differential expression under RNAi treatment.

284

285 The script performing these analyses is available in this project's code repository at
286 *offgenes_straintreatDE_deseq2_dnacov.R*.

287

288 *Gene set enrichment analysis*

289 We performed gene set enrichment analysis of genes differentially expressed upon RNAi
290 treatment using WormBase's enrichment analysis tool (Angeles-Albores et al., 2016; Harris et
291 al., 2020) (<https://wormbase.org/tools/enrichment/tea/tea.cgi>). We analyzed genes upregulated
292 and downregulated on each RNAi treatment in all five strains (20 analyses total; 5 strains x 2
293 treatments x 2 directions of differential expression). Upregulated genes were those with higher
294 expression on a treatment, with fold change > 1.5 vs control and adjusted p-value < 0.1 ;
295 downregulated genes were those with lower expression on a treatment, with fold change < -1.5
296 vs control and adjusted p-value < 0.1 (see 'Differential expression analysis'). The background
297 gene set for all analyses was the 18,529 genes included in overall differential expression
298 analyses. All gene-set enrichment related outputs were saved and the enrichment results tables
299 ('Download results table here') output were combined across strains for visualization.

300

301 The script performing this limited downstream processing is available in this project's code
302 repository at *exploreGeneSetEnrichmentResults.R*.

303

304 *High-performance computation*

305 Computationally intensive analyses were performed on the infrastructure of PACE (Partnership
306 for an Advanced Computing Environment), the high-performance computing platform at the
307 Georgia Institute of Technology. These analyses comprised pseudo-transcriptome generation,
308 expression quantification, DNA sequence coverage estimation, and their related computational
309 tasks.

310

311 *Figures and website*

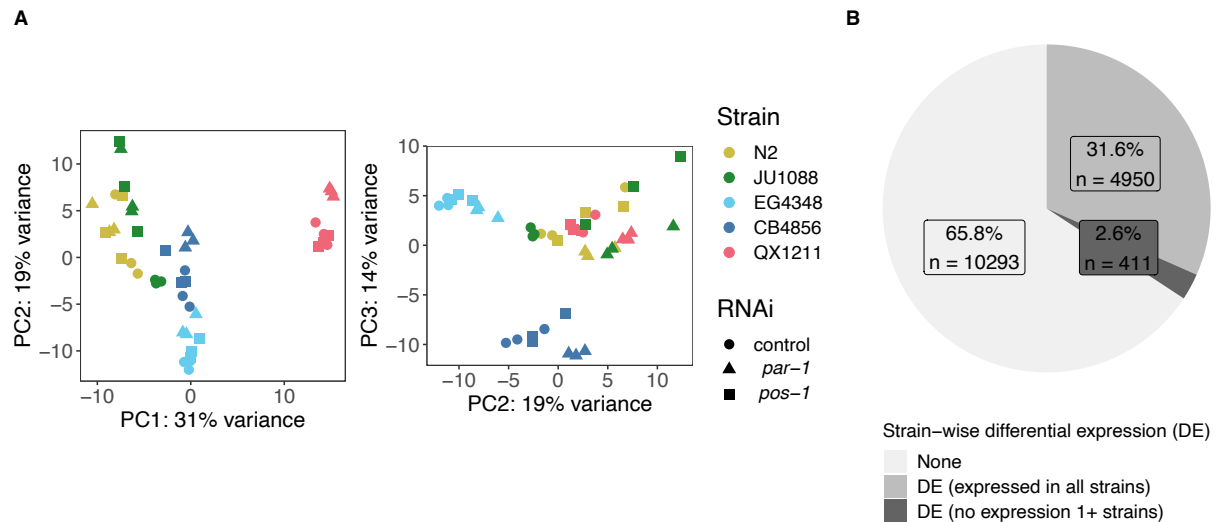
312 Figures were made in R (v4.1.0) (R Core Team, 2021) using packages ggplot2 (v3.3.6)
313 (Wickham, 2016), data.table (v1.14.3) (Dowle & Srinivasan, 2022) (<https://r-datatable.com>),
314 DESeq2 (v1.32.0) (Love et al., 2014), cowplot (v1.1.1) (Wilke, 2020), ggVennDiagram (v1.2.0)
315 (Gao, 2021), eulerr (v6.1.1) (Larsson, 2021), and ggpattern (v1.0.1) (FC et al., 2022), with color
316 schemes developed using RColorBrewer (v1.1-3) (Neuwirth, 2022) and Paul Tol's color palettes
317 (<https://personal.sron.nl/~pault/>). The interactive website that enables exploration of the data
318 from this study was developed using Shiny (Chang et al., 2022).

319

320 **Results and discussion**

321 To investigate natural variation in both gene expression and response to exogenous RNAi, we
322 performed RNA sequencing on five isogenic *C. elegans* strains in three conditions: RNAi
323 targeting the germline genes *par-1* and *pos-1* and the untreated condition. We included the
324 RNAi-competent reference strain N2 and four wild strains with varying competency to germline
325 RNAi (Paaby et al 2015, Chou et al 2022): JU1088 (highly competent), EG4348 (moderately
326 competent), and CB4856 and QX1211 (largely incompetent). These wild strains also vary in
327 divergence from N2, representing some of the least (JU1088) and most (QX1211) divergent
328 strains (variants per kilobase vs. N2 genome: 0.82, 1.40, 1.99, and 4.20, respectively, from
329 *Caenorhabditis elegans* Natural Diversity Resource [CeNDR] data (Cook et al., 2017)). To limit
330 bias arising from differences between non-N2 sequencing reads and the N2 reference genome
331 in our analysis, we first created strain-specific transcriptomes by inserting known single
332 nucleotide and insertion/deletion variants from CeNDR (Cook et al., 2017) into the reference
333 genome. Then, we pseudo-aligned the RNA reads to these strain-specific transcriptomes to

334 quantify per-gene RNA expression in each strain on each condition, and estimated differential
 335 expression based on strain, RNAi treatment, and their interaction.
 336



337
 338
 339 **Figure 1.** Genotype (strain) dominates expression variation across five *C. elegans* strains
 340 treated with RNAi targeting the genes *par-1* and *pos-1* or an empty vector control. **A)** Principal
 341 components analysis (PCA) of gene expression. PCs 1 vs. 2 (left) and 2 vs. 3 (right) of PCA of
 342 the 500 most variably expressed genes are plotted; the proportion of variance explained is
 343 noted on the axes. **B)** In the control condition, 34.2% of 15,654 nominally expressed genes are
 344 differentially expressed across strains (genome-wide adjusted $p < 0.1$ in a likelihood-ratio test
 345 between models including and excluding the *strain* term); a subset of these (approximately 2.6%
 346 overall) are not expressed at all in at least one strain (in any condition, see text for details).
 347 *Related Supplementary Material:*
 348 *File S1 contains the genes differentially expressed based on strain*
 349 *File S2 contains the ‘off’ genes identified as potentially unexpressed in one strain but expressed*
 350 *in others*

351
 352 **Genotype (strain)-wise expression variation predominates, nominates functionally**
 353 **diverged genes**

354 Overall, genotypic differences between strains explained more gene expression variation than
 355 RNAi treatment. We detected nominal expression at 18,589 genes across the full dataset; a
 356 principal components analysis of the 500 most variable genes shows distinct strain-wise
 357 partitioning of the variation (**Figure 1A**). To identify genes with significant expression differences
 358 between strains in just the control condition, we compared a model with a term for strain to one
 359 without (via a likelihood-ratio test) for each gene. Of the 15,654 genes included in this control-
 360 specific analysis, 5355, or approximately 34%, were differentially expressed across the five
 361 strains (likelihood-ratio test, genome-wide adjusted $p < 0.1$) (**File S1**). This fraction of genes
 362 with expression differences between strains is consistent with recent findings that 28% of

363 assayed genes were associated with mappable genetic differences (eQTLs) across 207 wild
364 strains (Zhang et al., 2022). Other systems, such as flies, also harbor extensive variation in
365 gene expression: a recent study of 200 inbred *Drosophila melanogaster* strains detected strain-
366 wise expression variation at the majority of genes (Everett et al., 2020). The experimental and
367 analytical approach matters a great deal; in the *Drosophila* study, many more variable genes
368 were identified using RNA-seq data than microarray data, and only 30-40% of differentially
369 expressed genes were associated with mappable eQTLs (Everett et al., 2020).

370

371 In some cases, presence versus absence of expression may underpin differential expression
372 across strains; this pattern could indicate strain-wise differences in functional requirements or in
373 developmental timing of expression. We identified such 'off' genes as those with zero mean
374 expression in at least one strain (across all conditions) as well as significant strain-wise
375 differential expression between a pair of strains in the control condition (genome-wide adjusted
376 $p < 0.1$). This conservative zero-read threshold reduces the frequency of misclassifying low
377 expression genes as off; the requirement for differential expression ensures true expression in
378 at least one strain. This stringent selection yielded 411 putative 'off' genes (**Figure 1B, File S2**).
379 Most of these genes lacked expression in a single strain: 249 were off in one strain, 105 were
380 off in two strains, 51 were off in three strains, and only 6 genes were expressed in a single
381 strain and off in the others (**Figure S1A**). We detected 49 genes that were off in N2 but
382 expressed in at least one other *C. elegans* strain. The complete functional repertoire of these
383 genes would therefore be invisible in a study using only the N2 strain. Such on/off patterns of
384 gene expression occur in other systems as well; for example, across 144 *Arabidopsis thaliana*
385 strains, thousands of genes showed strong expression in some strains but zero expression in
386 others (Zan et al., 2016).

387

388 To assess the potential significance of 'off' genes in the context of RNAi response, we
389 investigated whether any genes unexpressed in one strain exhibited differential expression
390 within another strain following *par-1* or *pos-1* RNAi treatment. Of the 411 'off' genes, 47 were
391 differentially expressed on an RNAi treatment in at least one other strain (RNAi differential
392 expression threshold: genome-wide adjusted $p < 0.1$ and fold change > 1.5 for within-strain
393 RNAi treatment vs. control comparisons) (**Figure S1B**). The majority ($n = 33$) of these genes
394 were differentially expressed in only one RNAi treatment in one strain. However, one gene
395 identified by this analysis is W06G6.11 (WBGene00012313), which was 'off' in N2 but
396 expressed in the other strains, and was significantly upregulated on RNAi against both *par-1*

397 and *pos-1* in RNAi-sensitive strain JU1088 (fold change = 1.9 and genome-wide adjusted p =
398 0.03; fold change = 3.4 and genome-wide adjusted p = 0.003, respectively). Prior RNA-seq and
399 microarray studies have indicated that W06G6.11 expression may be affected by the activity of
400 Argonaute *alg-1* (Aalto et al., 2018), a member of the RNA-induced silencing complex involved
401 in endogenous and exogenous short RNA processing (Grishok et al., 2001), and also by
402 exposure to pathogens (Engelmann et al., 2011; Lee et al., 2013). These studies detect
403 W06G6.11 expression in N2, but in samples derived from older adult hermaphrodites relative
404 the young adults we sampled; a study that included CB4856 also confirmed significantly higher
405 W06G6.11 expression in that strain relative to N2 (Zamanian et al., 2018).

406

407 This process of identifying genes that are unexpressed in some strains, but differentially
408 expressed based on a treatment or phenotype of interest in others, might be used to identify
409 candidate genes for other naturally variable phenotypes, perhaps as a complement to genotype-
410 to-phenotype mapping by genome-wide association studies with expression mediation analyses
411 (Evans & Andersen, 2020; Zhang et al., 2022).

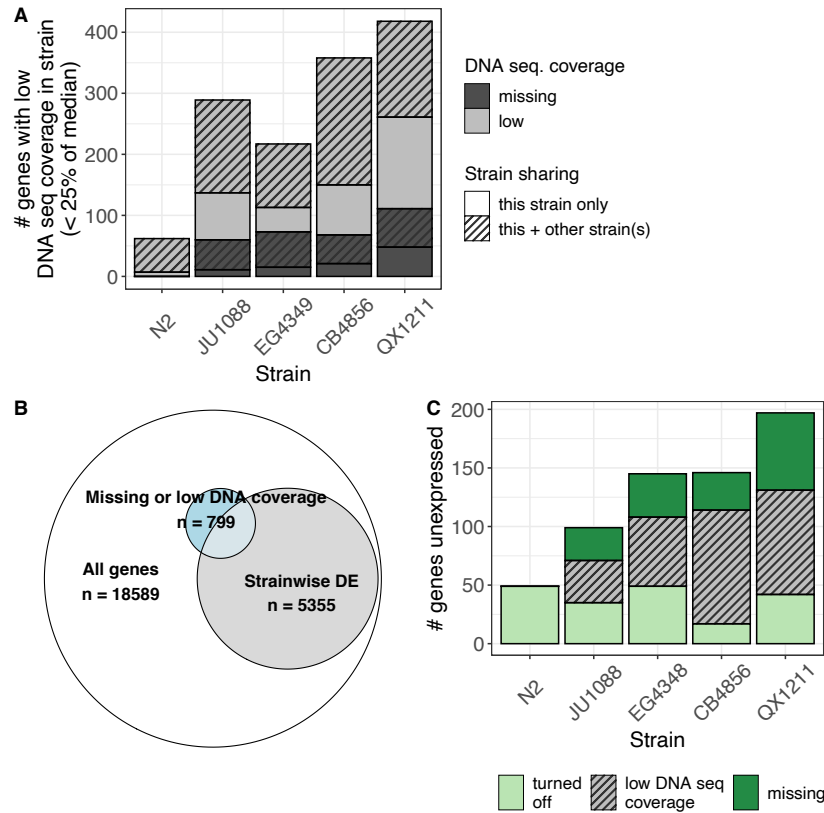
412

413 **Reference bias screening increases confidence in differential expression calls**

414 For RNA-seq studies that evaluate wild strains, reliance on a reference strain poses a concern.
415 The main issue is whether the mapping of fewer non-reference strain RNA reads than
416 reference-strain reads to a gene arise from true differences in gene expression, or from failure
417 of non-reference reads to correctly map to the reference genome due to sequence divergence
418 (reference bias) (Degner et al., 2009). Such discrepancies might remain even after the use of
419 genotype-specific transcriptomes. In the case of *C. elegans*, wild strains exhibit a wide range in
420 levels of divergence from the reference strain N2 in the species generally and the strains
421 studied here specifically (Andersen et al., 2012; Cook et al., 2017; Crombie et al., 2019); much
422 of this diversity is located in hyper-divergent haplotypes encompassing 20% of the genome (Lee
423 et al., 2021).

424

425 To refine our level of confidence in the genes we identified as differentially expressed, we
426 examined our results in the context of alignment quality in the original CeNDR genome
427 sequencing data (Cook et al., 2017) (**Figure S2, Files S3, S4**). For each strain in our study, we
428 curated a list of genes with missing or poor DNA sequence alignment in CeNDR (Cook et al.,
429 2017) (**File S5**). Specifically, we classified genes with exactly zero coverage as missing in that
430 strain's genome; this is a conservative assignment, as even one well-aligned DNA sequence



431
432

433 **Figure 2.** Improving confidence in differential expression calls by integrating DNA alignment
434 data. **A)** The number of genes with low (<25% of the median) and missing (zero raw coverage)
435 DNA alignment coverage (from CeNDR sequencing (Cook et al., 2017)) in each strain, of the
436 18,589 genes included in the expression analysis. Strain note: CeNDR assessed DNA coverage
437 in EG4349, the genetically identical isotype to EG4348. **B)** The total number of genes
438 differentially expressed based on strain (likelihood-ratio test of models including and excluding
439 *strain* term, genome-wide adjusted $p < 0.1$) and their overlap with genes classified as missing or
440 low DNA coverage in any strain (417 are both differentially expressed across strains and low
441 DNA coverage, hypergeometric enrichment test $p = 9.8 \times 10^{-46}$). Areas are proportional to
442 number of observations. **C)** The number of unexpressed 'off' genes per strain, subset into three
443 categories: called as turned off at the RNA level with high confidence; missing in the strain
444 genome (zero raw coverage); called with uncertainty, given low DNA sequence coverage (<25%
445 but >0 median DNA coverage).

446 *Related Supplementary Material:*

447 *Figure S2 shows DNA coverage distributions and cutoffs*

448 *File S2 contains details on each 'off' gene*

449 *File S3 contains raw per-gene DNA sequence coverage estimates*

450 *File S4 contains median-normalized per-gene DNA sequence coverage estimates*

451 *Files S5 contains the list of genes flagged as low DNA coverage*

452 *Files S6-7 provide numerical summaries of 'off' genes*

453

454 read precluded a gene from being classified as missing. We classified genes with more than
455 zero coverage but less than 25% of the gene-wise median DNA coverage in each strain as low
456 coverage. This process identified a similar set of genes across strains despite the contribution of

457 some strain-to-strain coverage variation (**Figure S2, File S5**). In total, we identified 799 genes
458 as missing or low DNA coverage in one or more strains (**Figure 2A**).

459

460 Were differentially expressed genes associated with poor DNA coverage? Overall, yes: overlap
461 of the missing-or-low coverage and strain-wise differentially expressed gene sets revealed
462 significant enrichment (hypergeometric test of enrichment $p = 9.8 \times 10^{-46}$). However, the
463 absolute number of differential expression genes with poor DNA coverage was modest: only 4%
464 of all genes analyzed and 8% of genes with differential expression across strains had missing or
465 low DNA coverage (**Figure 2B**). Put another way, 52% of missing or low DNA coverage genes
466 were called as differentially expressed, while 29% of all analyzed genes were called as
467 differentially expressed. Further, we note that poor DNA coverage arises from several sources.
468 First, by chance, some genes will be low coverage simply due to stochastic variation in short-
469 read sequencing depth, as reflected in the 62 genes binned as low coverage in N2 mapped to
470 itself (**Figure 2A**). Second, sequence divergence between the mapped strain and the reference
471 genome could inhibit alignment (reference bias); this possibility motivates this analysis. Third,
472 the gene could be missing from the strain's genome while present in the N2 reference genome.
473 Not surprisingly, QX1211, the strain most diverged from the N2 reference genome, exhibits the
474 most missing and the most low coverage genes (**Figure 2A, File S6**).

475

476 The set of 'off' genes that show zero expression in some strains may be particularly vulnerable
477 to reference bias, for example if they were more likely to be pseudogenes in at least one strain.
478 In this scenario, poor DNA coverage may be conflated with true expression loss, as
479 accumulated mutations may lead both to poor DNA coverage and consequently poor RNA
480 alignment and to reduced expression through mutation-mediated defunctionalization. Here,
481 when genes are detected as unexpressed, we can make distinctions between 1) missing genes,
482 which we are reasonably confident do not exist in the strain genome; 2) genes for which we may
483 not trust the conclusion of zero expression because of low DNA coverage and potential bias in
484 RNA read mapping; and 3) true 'off' genes, which do not fall into either category and likely
485 represent unbiased expression differences at the RNA level. In this scheme, among the four
486 non-reference strains, 17-49 (12-35%) of the originally detected 'off' genes are likely truly turned
487 off, 28-66 (22-34%) appear missing from the strain genome, and 36-89 (36-66%) are
488 undetected for an unknown reason but have low DNA coverage and may be influenced by
489 reference bias (**Figure 2C, File S7**).

490

491 As we would expect, all 49 'off' genes in the reference strain N2 were classified as truly
492 unexpressed; none were missing or low coverage (**Figure 2C**). Of these, 22 are listed as
493 pseudogenes on WormBase (Harris et al., 2020), and may represent alleles that have been
494 pseudogenized in the N2 lineage but remain functional in other strains. One such candidate is
495 the Argonaute ZK218.8 (WBGene00013942), which is expressed in strains CB4856 and
496 QX1211 and may reflect functional diversification in RNAi processes across the population
497 (Chou et al., 2022). Of the 47 'off' genes with *par-1* or *pos-1* RNAi effects in another strain, a
498 large majority ($n = 39$, 83%) were missing in the genome or were associated with low DNA
499 coverage (**Figure S3**). This majority represents a slight enrichment relative to the proportion of
500 missing or low coverage genes within the complete set of 'off' genes (286/411 or 70%) (one-
501 sided proportion test with continuity correction: $\chi^2 = 3.05$, $df = 1$, $p = 0.04$). Enrichment of
502 genome divergence among RNAi-responsive 'off' genes supports the hypothesis that genes
503 associated with RNAi are evolving rapidly in *C. elegans* (Chou et al., 2022). By adding the
504 missing and low DNA coverage filters, we infer that, of genes with an RNAi effect in another
505 strain, zero (in N2) to 12 (in QX1211) were missing from the strain's genome and 1-6 genes per
506 strain were present but truly unexpressed at the RNA level. These genes might be the most
507 interesting candidates for downstream expression-based study. This set includes the putative
508 RISC-associated gene W06G6.11 (WBGene00012313) discussed above.

509
510 An alternative approach to handling reference bias is to side-step it by excluding transcripts
511 associated with known (Lee et al., 2021) hyper-divergent haplotypes (Zhang et al., 2022).
512 However, because 1) some genes in hyper-divergent regions had good DNA alignment with low
513 SNP density and others outside the regions had no DNA coverage, and 2) our study focuses
514 exclusively on genic regions, we chose a gene-level, strictly coverage-based approach for bias
515 screening. Still, a limitation of our approach (and most others) is that it cannot identify bias
516 associated with elevated RNA levels in diverged or duplicated haplotypes relative to the N2
517 haplotype. Such bias could occur if reads in non-reference strains come from a gene poorly
518 represented or missing in the reference, which are then spuriously assigned to an incorrect
519 gene with a better match. This type of bias is difficult to define, quantify, and exclude.
520 Additionally, as for any arbitrary threshold, our cutoff of < 25% median coverage likely produces
521 a mix of false positives and negatives, *i.e.*, genes with low DNA coverage but accurate RNA
522 alignments and genes above the coverage cutoff that are nevertheless skewed by reference
523 bias. While those interested in specific genes would therefore do well to interrogate them

524 further, the DNA coverage approach provides a useful quality control filter for initial analyses of
525 differential expression.

526

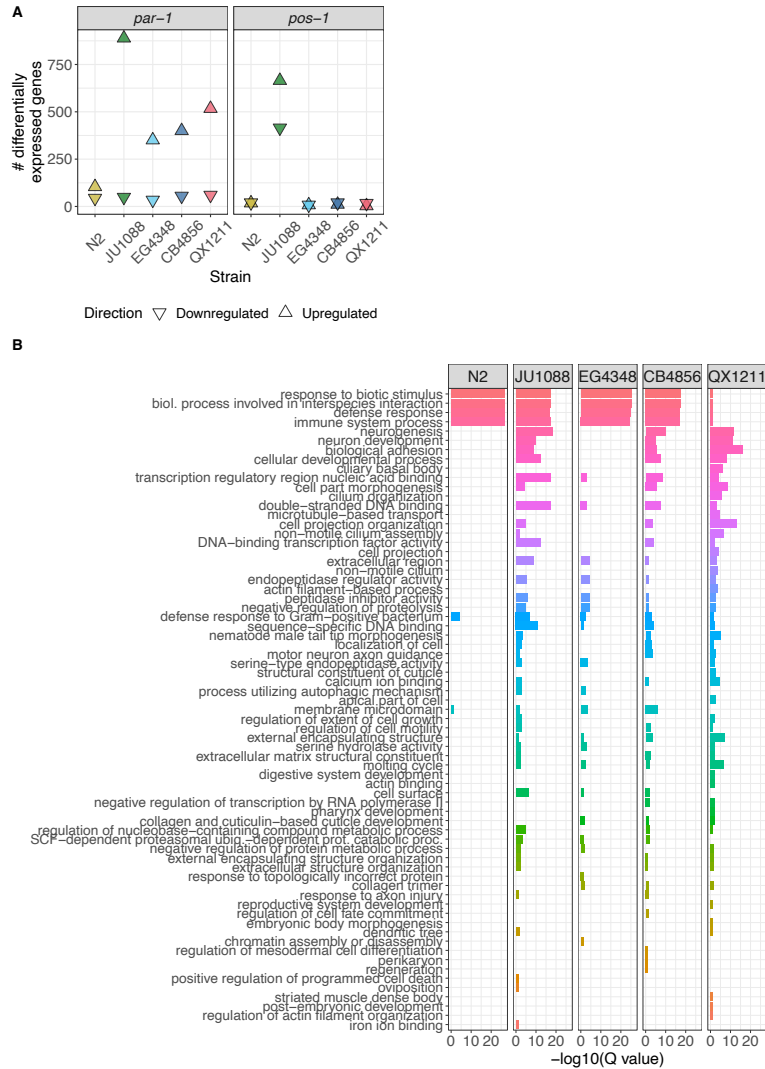
527 **Complex genotype and target specificity in transcriptional response to RNAi**

528 Wild *C. elegans* strains vary in response to exogenous RNA interference. In particular, strains
529 differ widely in competence for RNAi against germline targets delivered by feeding, as
530 measured by phenotypic consequences following putative target knockdown (Elvin et al., 2011;
531 Felix, 2008; Felix et al., 2011; Paaby et al., 2015; Tijsterman et al., 2002). To assess the
532 transcriptional response to RNAi in worms with variable germline RNAi competencies, we fed
533 worms dsRNA targeting the maternal-effect embryonic genes *par-1* and *pos-1* as well as the
534 empty vector control. Both genes are expressed in the mature hermaphrodite germline and are
535 essential for embryonic viability; in competent animals, RNAi by feeding results in dead embryos
536 (Paaby et al., 2015; Sijen et al., 2001). Gene expression knockdown of the targets themselves
537 confirmed the previously observed differences in RNAi competency (Chou et al., 2022; Paaby et
538 al., 2015): under *pos-1* RNAi, *pos-1* expression levels dropped the most in JU1088, followed by
539 N2 and then EG4348; strains CB4856 and QX1211 showed no drop in expression (**Figure S4A,**
540 **C**). RNAi against *par-1*, which induces a less lethal response (Chou et al., 2022; Paaby et al.,
541 2015), resulted in a similar though less strong pattern of *par-1* knockdown (**Figure S4B,D**).
542 These results confirm that strains differ in RNAi response and that the response was target-
543 gene-specific; this target specificity was also evident transcriptome-wide.

544

545 To assess how strains vary in overall transcriptional response to RNAi, we identified changes in
546 gene expression across treatments (*par-1* RNAi, *pos-1* RNAi, and the negative control) that
547 differed across the five strains. Specifically, for each gene in the dataset, we asked whether a
548 model with or without a strain x treatment interaction term better explained the pattern of
549 expression (see Methods). Genome-wide, 842 genes (5% of those assayed) varied in RNAi
550 response across strains (*i.e.*, had significant strain:treatment interaction via likelihood-ratio test,
551 genome-wide adjusted $p < 0.1$) (**File S8**). We also identified, within each strain, differences in
552 expression following *par-1* and *pos-1* RNAi relative to the control. The number of genes
553 differentially expressed under RNAi treatment (genome-wide adjusted $p < 0.1$, fold change $>$
554 1.5) varied substantially across strains and as well as between the two treatments (**Figure 3A,**
555 **Figure S5, Files S9a-j**).

556



557
 558 **Figure 3.** The transcriptional response to dsRNA is highly strain- and target-specific. **A)** The
 559 number of genes up- and down-regulated in each strain upon *par-1* and *pos-1* dsRNA
 560 ingestion/RNAi induction. Genes were called differentially expressed if their shrunken absolute
 561 fold change was > 1.5 and genome-wide adjusted p-value/FDR < 0.1. **B)** Gene set enrichment
 562 analysis results for genes upregulated on *par-1* dsRNA in each strain. Gene ontology (GO)
 563 categories that were significantly enriched (false discovery rate Q < 0.1) in any strain are
 564 included. GO terms are ranked and colored by median significance across strains.

565 *Related Supplementary Material:*
 566 *Figure S5 shows volcano plots for RNAi treatments for each strain*
 567 *Figure S6 contains Venn diagrams of overlap among strains in specific DE genes*
 568 *Figure S7 shows results from the same gene set enrichment analysis of genes downregulated*
 569 *under par-1 RNAi and up- and down-regulated under pos-1 RNAi*
 570 *Table S1 gives number of up and downregulated genes in each strain and included in each*
 571 *analysis*
 572 *File S8 contains the genes differentially expressed based on strain-treatment interaction*
 573 *Files S9a-j contain the genes differentially expressed in each strain in each RNAi treatment vs.*
 574 *control*
 575 *File S10 gives all enriched GO categories.*
 576

577 On both *par-1* and *pos-1* RNAi, the highly germline-RNAi competent strain JU1088 exhibited the
578 most differentially expressed genes relative to the control, suggesting that this strain is the most
579 transcriptionally responsive to RNAi (**Figure 3A, Figure S5**). However, on *par-1* RNAi, the
580 moderately competent strain EG4348 and the largely incompetent strains CB4856 and QX1211
581 showed substantially more differentially expressed genes than the competent laboratory strain
582 N2. These results indicate that the number of genes transcriptionally responsive to exogenous
583 RNAi is not predictive of RNAi phenotypic penetrance, and that ‘competence’ defined by end-
584 point phenotypes and/or artificial triggers may obscure intermediary RNAi activity, or activity in
585 alternative RNAi pathways (Chou et al., 2022).

586
587 Relative to *par-1*, *pos-1* RNAi induced substantially fewer differentially expressed genes in all
588 strains but JU1088, indicating that RNAi transcriptional response is highly target-specific.
589 Furthermore, differential expression following *par-1* RNAi was strongly skewed towards an
590 overabundance of upregulated genes compared to downregulated genes (**Figure 3A, Figure**
591 **S5**). Of course, a transcriptional response may reflect developmental consequences of losing
592 *par-1* or *pos-1* gene expression, at least in competent strains (Chou et al., 2022; Paaby et al.,
593 2015); here, we cannot easily distinguish these effects from those arising from induction of the
594 RNAi process itself. However, several lines of evidence suggest that RNAi process effects
595 dominate. First, RNAi is a systemic phenomenon with a repertoire of many genes (Billi et al.,
596 2014) while *par-1* and *pos-1* expression is largely restricted to the germline with consequential
597 effects predominantly in the early embryo (Harris et al., 2020); our samples were prepared from
598 whole worms. Second, the incompetent strains exhibited transcriptional responses genome-
599 wide, but not at the targeted genes. Finally, as described below, the transcriptional response at
600 a gene-by-gene level was strain-specific, consistent with our growing understanding of natural
601 variation in RNAi.

602
603 To identify transcriptional responses to RNAi that may be universal within *C. elegans*, we first
604 checked for differentially expressed genes that were shared across strains. However, overlap
605 among strains was sparse (**Figure S6**): no genes with differential expression to both *par-1* and
606 *pos-1* RNAi were shared across all five strains, and the only gene responsive to both treatments
607 in the competent strains (JU1088, N2, and EG4348) was *asp-14*, a predicted aspartyl protease
608 involved in innate immunity (Harris et al., 2020). Such strain-specific patterns fit with our
609 observations of RNAi variability: not only does *C. elegans* exhibit substantial natural variation in
610 germline RNAi competence (Elvin et al., 2011; Felix, 2008; Felix et al., 2011; Paaby et al., 2015;

611 Tijsterman et al., 2002), but the genetic basis for RNAi failure appears strain-specific as well
612 (Chou et al., 2022). We posit that even among competent strains, *C. elegans* varies in details of
613 the RNAi biological response mechanism, including which genes are affected, the magnitude or
614 functionality of their activity, and their timing. These differences are apparent in the
615 transcriptional responses of N2 and JU1088 (**Figure 3, Figure S6, Figure S7**), including the
616 activity of W06G6.11 described above. As the RNAi response is also highly target-specific,
617 these results portray RNAi as a phenomenon of exquisite specificity and context dependence.

618

619 However, statistical flux around significance cutoffs within strains may limit detection of gene-
620 specific responses, and we also wished to examine the biological significance of the
621 transcriptional responses. Therefore, we investigated whether the same general classes of
622 genes responded to RNAi across strains by applying WormBase gene set enrichment analyses
623 (Angeles-Albores et al., 2016; Harris et al., 2020) to the sets of genes up- and down-regulated
624 on the RNAi treatments (**Files S9**). Strains showed a clear pattern of enriched gene ontology
625 (GO) categories, particularly in the largest gene set, those upregulated under *par-1* RNAi
626 (**Figure 3B, File S10**). Specifically, GO terms associated with canonical RNAi functions such as
627 immune defense were well represented in all strains except in the germline incompetent strain
628 QX1211, and genes in other categories were enriched in all strains except in N2. This pattern
629 explains the paucity of differentially expressed genes in N2 relative to other strains following
630 *par-1* RNAi (**Figure 3A**), as those in N2 are restricted to immunity associated ontology. These
631 results demonstrate that reference strain N2 may not be a good representative for RNAi
632 transcriptional response in *C. elegans* generally. Some of these patterns were also evident at
633 genes downregulated under *par-1* RNAi, and up- and down-regulated under *pos-1* RNAi, though
634 these results were less clear (**Figure S7**); this difference from *par-1* upregulated genes might
635 reflect the more limited pool of differentially expressed genes in those categories.

636

637 In sum, transcriptional responses to RNAi differed across strains, but these responses did not
638 clearly discriminate between RNAi competent and incompetent strains in the context of N2-
639 derived GO categories: some competent strains upregulated non-defense categories while N2
640 did not, and incompetent strain CB4856 upregulated defense categories while incompetent
641 strain QX1211 did not. That said, some strain-specific aspects of RNAi responses at the
642 phenotype level may shed light on the transcriptional response enrichments. EG4348 is partially
643 sensitive to RNAi (Chou et al., 2022; Felix et al., 2011; Paaby et al., 2015), and its GO term
644 profile is similar to highly sensitive strain JU1088. While largely incompetent for germline RNAi,

645 CB4856 does eventually exhibit strong RNAi phenotypes at late ages (Chou et al., 2022; Felix
646 et al., 2011; Paaby et al., 2015; Tijsterman et al., 2002); its GO term profile similarity to JU1088
647 could be explained by the fact that this delay arises from the perturbation of a single gene, *ppw-*
648 *1* (Tijsterman et al., 2002). Alternatively, QX1211 exhibits an apparent on/off response pattern
649 among individual animals (Chou et al., 2022), and this binary penetrance of may be insufficient
650 to detect defense/immune gene upregulation in a bulk analysis.

651

652 **A public web resource for data exploration**

653 We have built a user-friendly, interactive website (<https://wildworm.biosci.gatech.edu/rnai/>) to
654 enable straightforward public exploration of our gene expression data across the five wild *C.*
655 *elegans* strains and three RNAi conditions. For any gene in our analysis, this website 1)
656 visualizes the RNA quantification per sample split by treatment or strain, 2) allows the user to
657 look up differential expression results between any two strain-treatment groups, 3) reports if
658 expression differs by strain in the control condition and by RNAi treatment across strains, and 4)
659 enables initial reference bias screening by displaying DNA sequencing coverage and whether
660 the gene overlaps a hyperdivergent haplotype. This website may be useful for exploratory
661 analyses of genes of interest for many types of studies in the *C. elegans* community.

662

663 **Conclusion**

664 The results of the investigations described here further expand our understanding of *C. elegans*
665 processes beyond the reference strain N2. Our quantification of gene expression variation
666 among wild strains demonstrates that mapping bias arising from the use of a reference genome,
667 while a greater liability for inferences about individual genes, can be restricted to a relatively
668 minor concern for genome-wide studies in this system. However, the strain-specific variation in
669 RNAi transcriptomic response suggests that our understanding of RNAi processes, derived
670 predominantly from studies in N2, incompletely represents RNAi biology in *C. elegans* as a
671 whole. The type of dataset presented here, genome-wide expression in multiple natural genetic
672 backgrounds over multiple conditions of interest, enables researchers to characterize how much
673 variation exists in the experimental systems we study. Understanding the scope of natural
674 variation informs evolutionary hypotheses about traits of interest and offers insight into
675 otherwise inaccessible relationships among genes, their functions, and phenotypes.

676 [Data availability](#)

677 Strains and feeding vectors are available from CeNDR or the CGC, and upon request. All
678 supplementary data files are available via Zenodo at <https://doi.org/10.5281/zenodo.7406794>:
679 File S1 contains the genes differentially expressed based on strain; File S2 contains the ‘off’
680 genes identified as potentially unexpressed in one strain but expressed in others; File S3
681 contains raw per-gene DNA sequence coverage estimates; File S4 contains median-normalized
682 per-gene DNA sequence coverage estimates; File S5 contains the list of genes flagged as low
683 DNA coverage; Files S6-7 contain summaries of missing/zero coverage genes; File S8 contains
684 the genes differentially expressed based on strain-treatment interaction; Files S9a-j contain the
685 genes differentially expressed in each strain in each RNAi treatment vs. control; File S10
686 contains the results of the gene set enrichment analyses. Per-gene differential testing results
687 and related information are available via an interactive web app at
688 <https://wildworm.biosci.gatech.edu/rnai/>. Gene expression data (raw and processed) are
689 available at GEO with the accession number GSE19083. Code used for all analyses can be
690 found at <https://github.com/averydavisbell/wormstrainrnaiepr>.

691

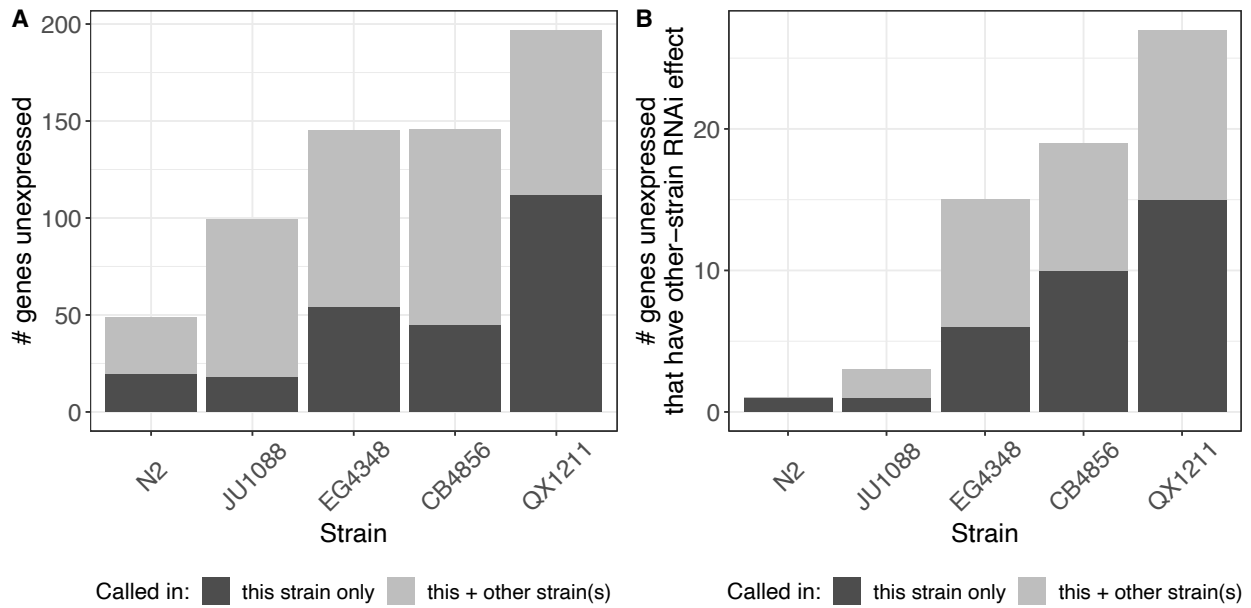
692 [Acknowledgments](#)

693 We are grateful to members of the Paaby lab for helpful conversations about this work. We
694 appreciate the use of the shared equipment, services, and expertise of the core facilities at the
695 Parker H. Petit Institute for Bioengineering and Bioscience at the Georgia Institute of
696 Technology. Specifically, we thank Shweta Biliya at the Molecular Evolution Core for
697 collaboration on sequencing. Troy Hilley provided expert web server configuration support for
698 the interactive web app. This research was supported in part through research
699 cyberinfrastructure resources and services provided by the Partnership for an Advanced
700 Computing Environment (PACE) at the Georgia Institute of Technology, Atlanta, Georgia, USA.
701 As ever, WormBase served as an invaluable resource to this study. This research was funded
702 by NIH grant R35 GM119744 to A.B.P. and NSF Postdoctoral Research Fellowship in Biology
703 2109666 to A.D.B.

704

705 **Supplementary Figures**

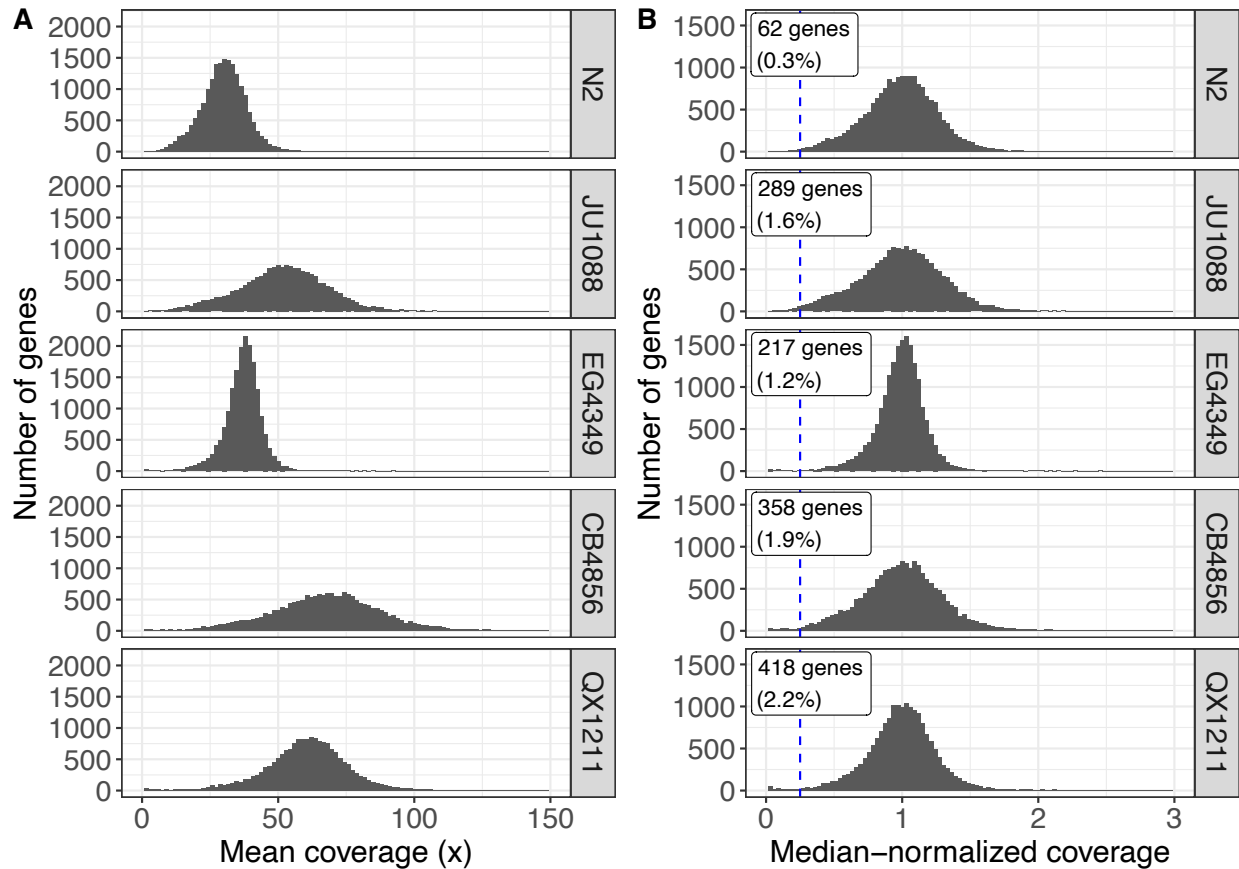
706



707

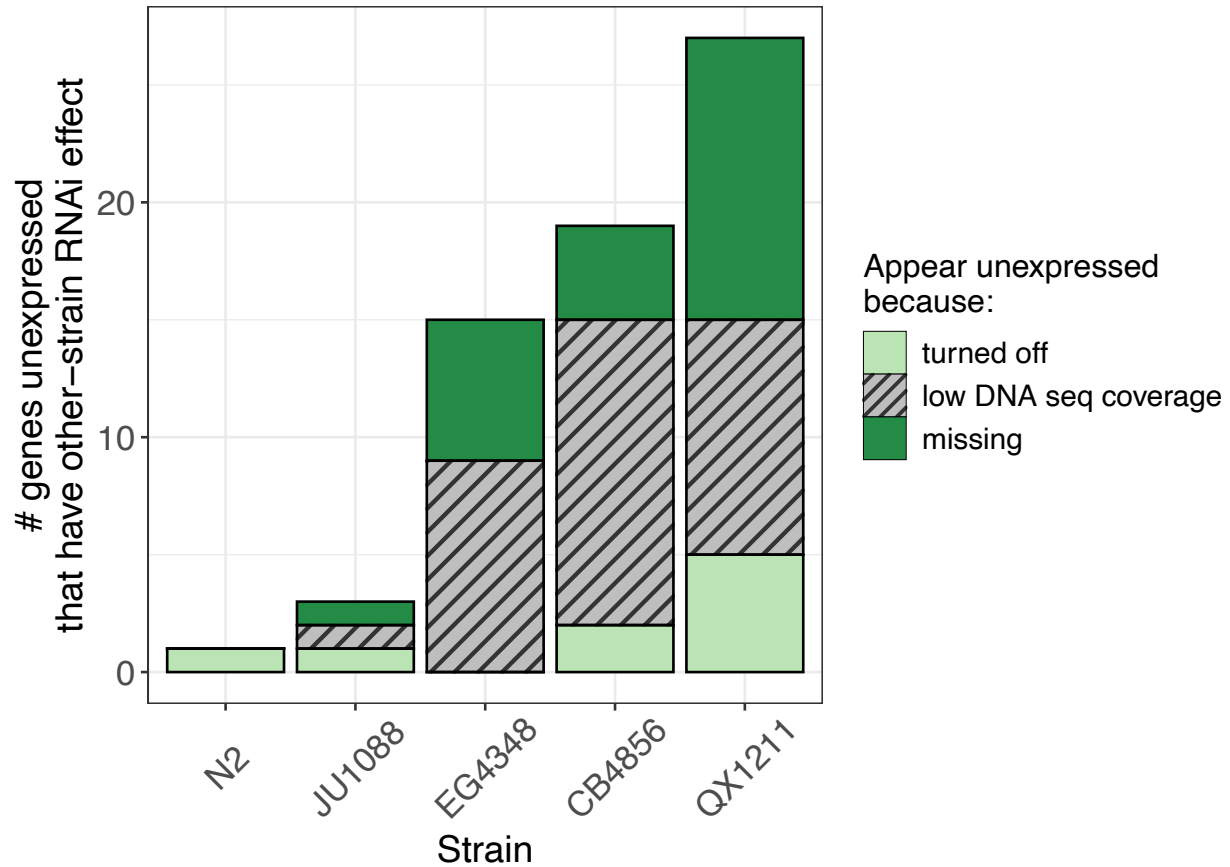
708

709 **Figure S1.** 'Off' genes, which are expressed in at least one strain but show no expression in
710 one or more others. **A)** All 'off' genes per strain, either unique or shared across strains (n = 411
711 total; genes may be present for multiple strains). **B)** The subset of 'off' genes that exhibit
712 differential expression on RNAi to *par-1* or *pos-1* in other strains, which are potential candidates
713 for RNAi functional divergence (n = 47 total; genes may be present for multiple strains).
714 *File S2 contains identity and details for each of these 'off' genes.*



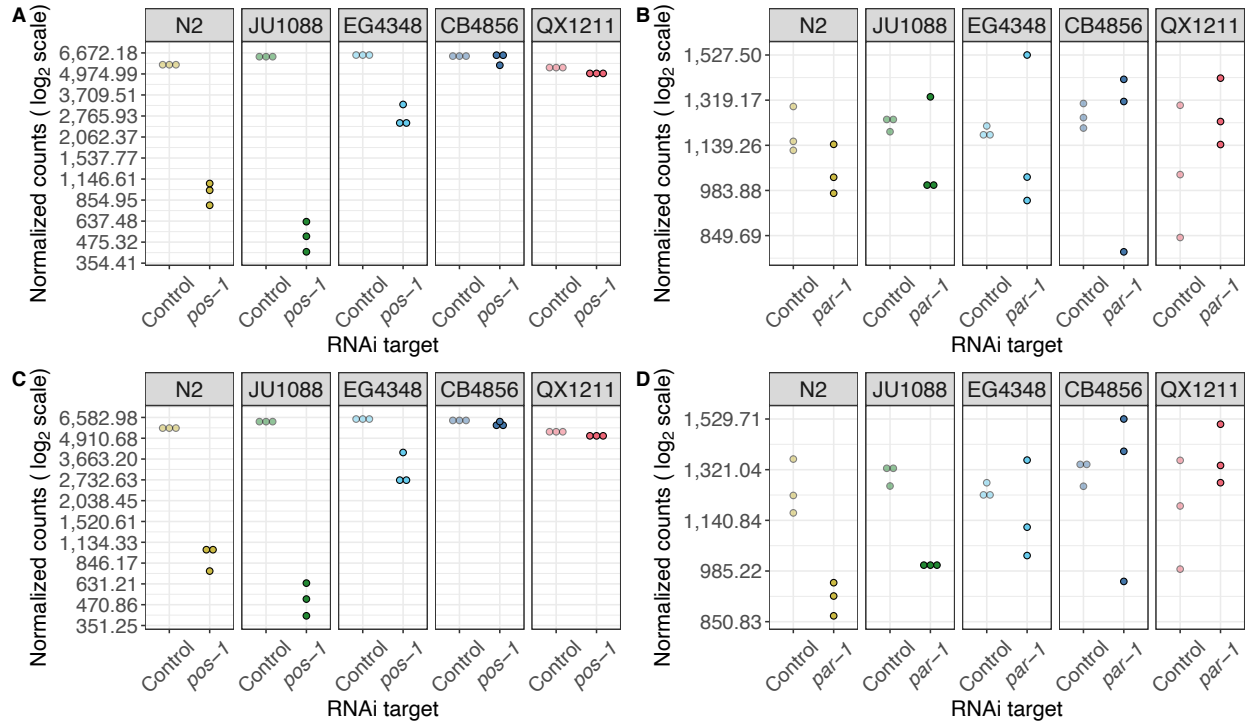
715
716

717 **Figure S2.** DNA sequence coverage across 18,589 genes included in expression analyses.
718 Aligned DNA sequence data was obtained from CeNDR (release 20210121) (Cook et al., 2017).
719 **A)** Mean coverage (mean number of reads covering each base) over merged non-overlapping
720 exonic regions of genes in the five strains in this study. CeNDR assessed DNA coverage in
721 EG4349, the genetically identical isotype to EG4348. The x-axis is truncated at 150x coverage
722 for visual clarity, excluding 179 genes across all strains combined. **B)** Median-normalized
723 coverage for the same genes as in **(A)**. Genes with less than 25% median coverage are
724 considered low DNA coverage in this study; this boundary is demarcated with the blue dashed
725 line and the number and proportion of genes this set comprises is noted on the plots. The x-axis
726 is truncated at 3x median coverage for visual clarity, excluding 227 genes across all strains
727 combined.
728 *Files S3 and S4 contain the source data. File S5 provides the list of genes identified as low*
729 *coverage.*



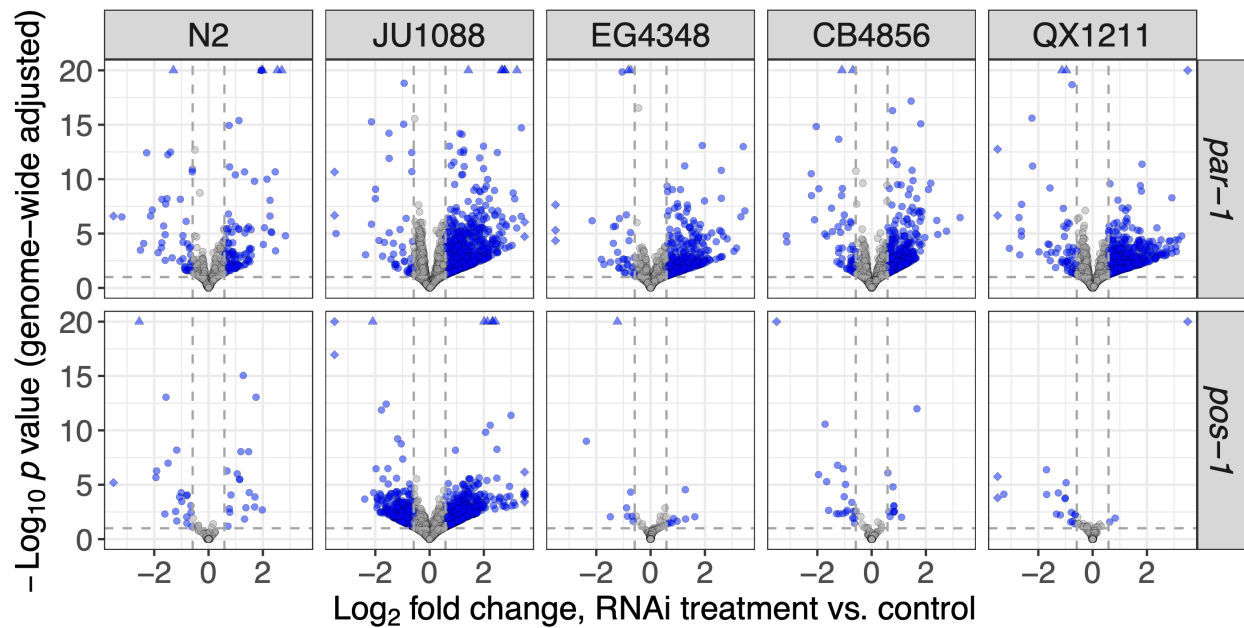
730
731
732
733
734
735
736
737

Figure S3. 'Off' genes that were unexpressed in one or more strains but differentially expressed with respect to *par-1* or *pos-1* RNAi in another strain, potential candidates for RNAi functional divergence. DNA sequence coverage information is denoted with color and shading. Missing genes were those with zero DNA sequence coverage; low DNA sequence coverage genes had greater than zero but less than 25% median gene's coverage; genes classified as truly turned off had greater than 25% median gene's DNA sequence coverage. (DNA coverage was assessed in strain EG4349, isotype to EG4348).



738
739

740 **Figure S4.** RNA-seq estimates suggest RNAi targets are knocked down commensurate with
741 each strain's RNAi capacity. **(A and B)** Quantification estimates from pseudoalignment to strain-
742 specific transcriptomes, normalized to library size and gene length, as used for all analyses in
743 this study. **A)** Quantification estimates for *pos-1* in control and exposure to *pos-1* dsRNA;
744 response is significantly different across strains (the strain:treatment interaction is significant,
745 genome-wide adjusted $p = 4 \times 10^{-254}$). **B)** Quantification estimates for *par-1* in control and
746 exposure to *par-1* dsRNA (the strain:treatment interaction is not significant, genome-wide
747 adjusted $p = 0.92$). **(C and D)** Detection of target knockdown is not dependent on RNAi
748 strategy: panels show *pos-1* and *par-1* quantification estimates as in **(A and B)**, respectively,
749 but with alternative expression estimates derived from RNA sequence data uniquely mapping to
750 one genomic location when containing the reference or non-reference allele (see methods).

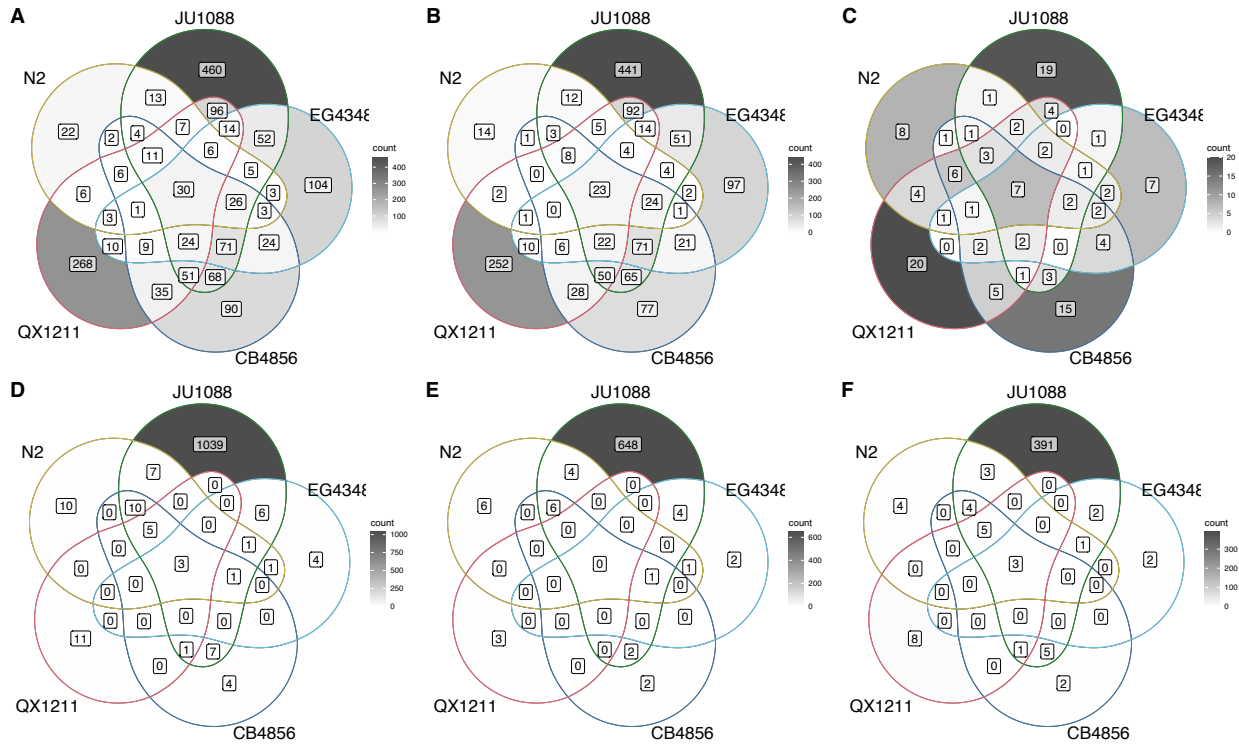


Point shape reflects if value is beyond plot area:

- ◇ Absolute value(log_2 fold change) > 3.5
- △ $p < 1 \times 10^{-20}$
- [all others]

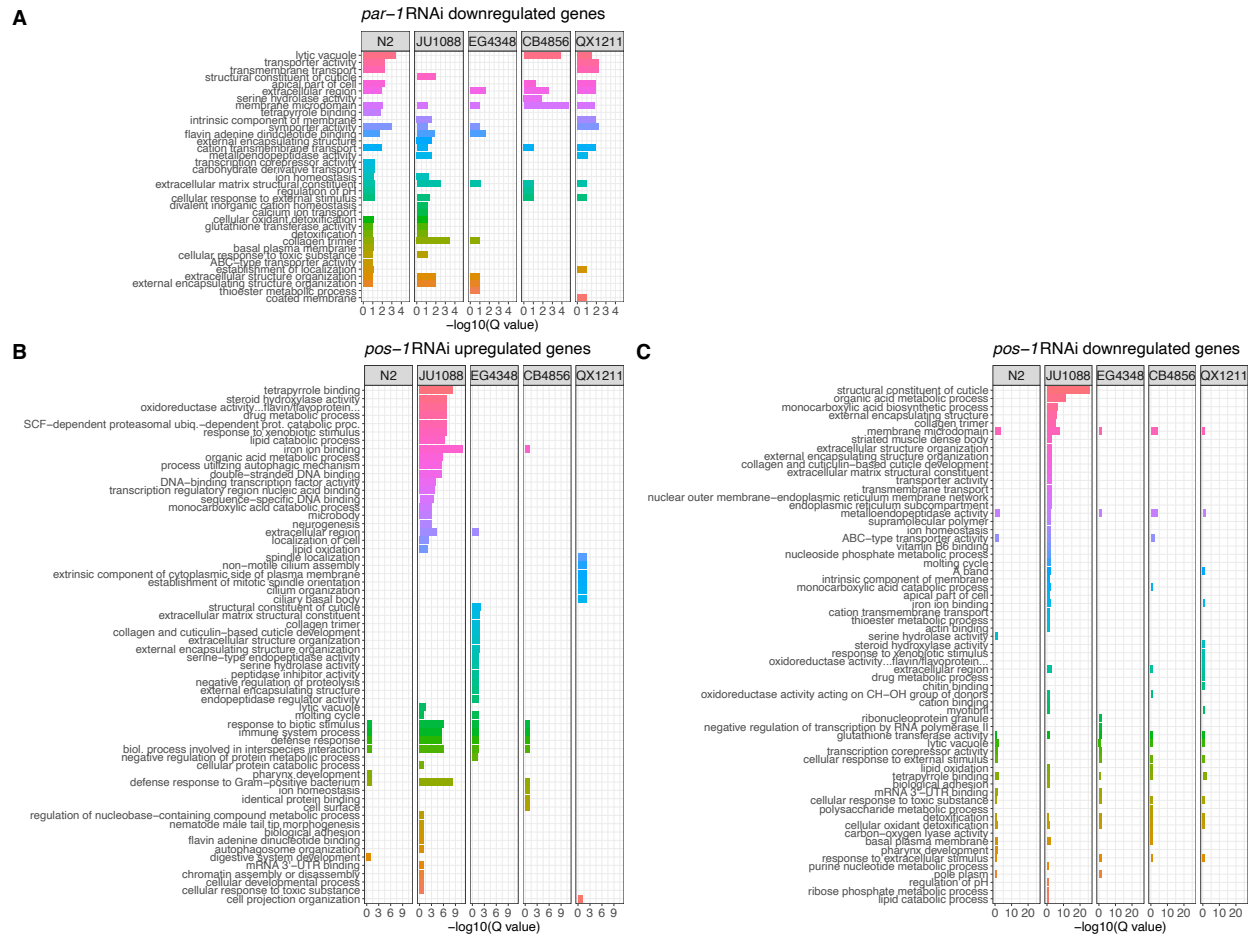
751
752
753
754
755
756
757
758
759
760
761

Figure S5. Volcano plots show genome-wide effects of RNAi treatments (against *par-1*, top, and *pos-1*, bottom) in each of the five strains. All genes with differential expression estimates are plotted; blue points denote genes with significant differential expression (genome-wide adjusted $p < 0.1$ and corrected [see methods] absolute value(fold change) > 1.5; these thresholds are annotated on the plot with gray dashed lines). For visual clarity, the y-axis is truncated at $p = 10^{-20}$ and the x-axis is truncated at absolute log_2 fold change = 3.5; genes with values exceeding these thresholds are included on the plots and are represented by unique point shapes as noted in the plot legend.



762
763

764 **Figure S6.** Limited overlap of genes called as differentially expressed in RNAi conditions vs.
765 control across strains; shading scales with number of genes separately within each panel (see
766 color bar legends). (A-C) Under *par-1* RNAi, genes differentially expressed in either direction
767 (A), upregulated (B), or downregulated (C). (D-F) Under *pos-1* RNAi, genes differentially
768 expressed in either direction (D), upregulated (E), or downregulated (F). Genes were called
769 differentially expressed and included if their shrunken absolute fold change was > 1.5 and
770 genome-wide adjusted p-value/FDR < 0.1 between RNAi and control within-strain.
771 Files S9a-j contain gene IDs and details. Figure 3A and Table S1 show the overall number of
772 up- and down-regulated genes in each strain.



773
774
775
776
777
778
779
780

Figure S7. Gene set enrichment analysis results for genes (A) downregulated on *par-1* dsRNA in each strain, (B) upregulated on *pos-1* dsRNA, and (C) downregulated on *par-1* dsRNA. Only gene ontology (GO) categories significantly enriched (FDR $Q < 0.1$) in upregulated genes in any strain are included. GO terms are ranked and colored by median significance across strains. Table S1 provides the number of genes included for each analysis. File S10 gives all enriched GO categories. Main Fig 3B displays the same analysis of genes upregulated under *par-1* RNAi.

781 **Supplementary Tables**

782

783 **Table S1.** The number of genes differentially expressed in each RNAi treatment in each strain,
 784 relative to the control condition, as well as the number included in the gene set enrichment
 785 analysis (GSEA).

RNAi Treatment	Strain	Up- or down-regulated vs. control-treated samples	N genes significantly up- or downregulated*	N genes included in GSEA testing	N genes excluded from GSEA testing**	
<i>par-1</i>	CB4856	Down	55	35	20	
		Up	400	282	118	
	EG4348	Down	34	22	12	
		Up	351	222	129	
	JU1088	Down	49	29	20	
		Up	909	569	340	
	N2	Down	44	31	13	
		Up	104	62	42	
	QX1211	Down	60	46	14	
		Up	517	380	137	
	<i>pos-1</i>	CB4856	Down	20	17	3
			Up	11	5	6
EG4348		Down	8	7	1	
		Up	8	6	2	
JU1088		Down	415	315	100	
		Up	665	394	271	
N2		Down	20	16	4	
		Up	18	7	11	
QX1211		Down	17	15	2	
		Up	3	2	1	

786

787 Literature Cited

- 788 Aalto, A. P., Nicastro, I. A., Broughton, J. P., Chipman, L. B., Schreiner, W. P., Chen, J. S., &
789 Pasquinelli, A. E. (2018, Jun). Opposing roles of microRNA Argonautes during
790 *Caenorhabditis elegans* aging. *PLoS Genet*, 14(6), e1007379.
791 <https://doi.org/10.1371/journal.pgen.1007379>
792
- 793 Ahringer, J. (2006). Reverse genetics. In V. Ambros (Ed.), *WormBook*.
794 <https://doi.org/doi/10.1895/wormbook.1.47.1>
795
- 796 Andersen, E. C., Gerke, J. P., Shapiro, J. A., Crissman, J. R., Ghosh, R., Bloom, J. S., Felix, M.
797 A., & Kruglyak, L. (2012, Jan 29). Chromosome-scale selective sweeps shape
798 *Caenorhabditis elegans* genomic diversity. *Nat Genet*, 44(3), 285-290.
799 <https://doi.org/10.1038/ng.1050>
800
- 801 Andersen, E. C., & Rockman, M. V. (2022, Jan 4). Natural genetic variation as a tool for
802 discovery in *Caenorhabditis* nematodes. *Genetics*, 220(1).
803 <https://doi.org/10.1093/genetics/iyab156>
804
- 805 Angeles-Albores, D., RY, N. L., Chan, J., & Sternberg, P. W. (2016, Sep 13). Tissue enrichment
806 analysis for *C. elegans* genomics. *BMC Bioinformatics*, 17(1), 366.
807 <https://doi.org/10.1186/s12859-016-1229-9>
808
- 809 Barriere, A., & Felix, M. A. (2005, Jul 12). High local genetic diversity and low outcrossing rate in
810 *Caenorhabditis elegans* natural populations. *Curr Biol*, 15(13), 1176-1184.
811 <https://doi.org/10.1016/j.cub.2005.06.022>
812
- 813 Barriere, A., & Felix, M. A. (2005). Natural variation and population genetics of *Caenorhabditis*
814 *elegans*. *WormBook*. <https://doi.org/10.1895/wormbook.1.43.1>
815
- 816 Bendesky, A., Pitts, J., Rockman, M. V., Chen, W. C., Tan, M. W., Kruglyak, L., & Bargmann, C.
817 I. (2012). Long-range regulatory polymorphisms affecting a GABA receptor constitute a
818 quantitative trait locus (QTL) for social behavior in *Caenorhabditis elegans*. *PLoS Genet*,
819 8(12), e1003157. <https://doi.org/10.1371/journal.pgen.1003157>
820
- 821 Billi, A. C., Fischer, S. E. J., & Kim, J. K. (2014). Endogenous RNAi pathways in *C. elegans*.
822 *WormBook*. <https://doi.org/10.1895/wormbook.1.170.1>
823
- 824 Bolger, A. M., Lohse, M., & Usadel, B. (2014, Aug 1). Trimmomatic: a flexible trimmer for
825 Illumina sequence data. *Bioinformatics*, 30(15), 2114-2120.
826 <https://doi.org/10.1093/bioinformatics/btu170>
827
- 828 Chang, W., Cheng, J., Allaire, J., Sievert, C., Schloerke, B., Xie, Y., Allen, J., McPherson, J.,
829 Dipert, A., & Borges, B. (2022). shiny: Web Application Framework for R.
830 <https://CRAN.R-project.org/package=shiny>
831
- 832 Chou, H. T., Valencia, F., Alexander, J. C., Bell, A. D., Deb, D., Pollard, D. A., & Paaby, A. B.
833 (2022). Diversification of small RNA pathways underlies germline RNAi incompetence in
834 wild *C. elegans* strains. *bioRxiv*, 2021.2008.2021.457212.
835 <https://doi.org/10.1101/2021.08.21.457212>
836

- 837 Cook, D. E., Zdraljevic, S., Roberts, J. P., & Andersen, E. C. (2017, Jan 4). CeNDR, the
838 Caenorhabditis elegans natural diversity resource. *Nucleic Acids Res*, 45(D1), D650-
839 D657. <https://doi.org/10.1093/nar/gkw893>
840
- 841 Corsi, A. K., Wightman, B., & Chalfie, M. (2015). A Transparent window into biology: A primer
842 on Caenorhabditis elegans. *WormBook*. <https://doi.org/doi/10.1895/wormbook.1.177.1>
843
- 844 Crombie, T. A., Zdraljevic, S., Cook, D. E., Tanny, R. E., Brady, S. C., Wang, Y., Evans, K. S.,
845 Hahnel, S., Lee, D., Rodriguez, B. C., Zhang, G., van der Zwagg, J., Kiontke, K., &
846 Andersen, E. C. (2019, Dec 3). Deep sampling of Hawaiian Caenorhabditis elegans
847 reveals high genetic diversity and admixture with global populations. *Elife*, 8.
848 <https://doi.org/10.7554/eLife.50465>
849
- 850 Degner, J. F., Marioni, J. C., Pai, A. A., Pickrell, J. K., Nkadori, E., Gilad, Y., & Pritchard, J. K.
851 (2009, Dec 15). Effect of read-mapping biases on detecting allele-specific expression
852 from RNA-sequencing data. *Bioinformatics*, 25(24), 3207-3212.
853 <https://doi.org/10.1093/bioinformatics/btp579>
854
- 855 Dilks, C. M., Koury, E. J., Buchanan, C. M., & Andersen, E. C. (2021, Dec). Newly identified
856 parasitic nematode beta-tubulin alleles confer resistance to benzimidazoles. *Int J*
857 *Parasitol Drugs Drug Resist*, 17, 168-175. <https://doi.org/10.1016/j.ijpddr.2021.09.006>
858
- 859 Dowle, M., & Srinivasan, A. (2022). data.table: Extension of `data.frame`.
860 <https://Rdatatable.gitlab.io/data.table>
861
- 862 Elvin, M., Snoek, L. B., Frejno, M., Klemstein, U., Kammenga, J. E., & Poulin, G. B. (2011, Oct
863 17). A fitness assay for comparing RNAi effects across multiple C. elegans genotypes.
864 *BMC Genomics*, 12, 510. <https://doi.org/10.1186/1471-2164-12-510>
865
- 866 Engelmann, I., Griffon, A., Tichit, L., Montanana-Sanchis, F., Wang, G., Reinke, V., Waterston,
867 R. H., Hillier, L. W., & Ewbank, J. J. (2011). A comprehensive analysis of gene
868 expression changes provoked by bacterial and fungal infection in C. elegans. *PLOS*
869 *ONE*, 6(5), e19055. <https://doi.org/10.1371/journal.pone.0019055>
870
- 871 Evans, K. S., & Andersen, E. C. (2020). The Gene *scb-1* Underlies Variation in *Caenorhabditis*
872 *elegans* Chemotherapeutic Responses. *G3: Genes|Genomes|Genetics*, 10(7), 2353-
873 2364. <https://doi.org/10.1534/g3.120.401310>
874
- 875 Evans, K. S., van Wijk, M. H., McGrath, P. T., Andersen, E. C., & Sterken, M. G. (2021, Oct).
876 From QTL to gene: C. elegans facilitates discoveries of the genetic mechanisms
877 underlying natural variation. *Trends Genet*, 37(10), 933-947.
878 <https://doi.org/10.1016/j.tig.2021.06.005>
879
- 880 Evans, K. S., Wit, J., Stevens, L., Hahnel, S. R., Rodriguez, B., Park, G., Zamanian, M., Brady,
881 S. C., Chao, E., Introcaso, K., Tanny, R. E., & Andersen, E. C. (2021, Mar). Two novel
882 loci underlie natural differences in Caenorhabditis elegans abamectin responses. *PLoS*
883 *Pathog*, 17(3), e1009297. <https://doi.org/10.1371/journal.ppat.1009297>
884
- 885 Everett, L. J., Huang, W., Zhou, S., Carbone, M. A., Lyman, R. F., Arya, G. H., Geisz, M. S., Ma,
886 J., Morgante, F., St Armour, G., Turlapati, L., Anholt, R. R. H., & Mackay, T. F. C. (2020,

- 887 Mar). Gene expression networks in the Drosophila Genetic Reference Panel. *Genome*
888 *Res*, 30(3), 485-496. <https://doi.org/10.1101/gr.257592.119>
889
- 890 FC, M., Davis, T. L., & ggplot2 authors. (2022). ggpattern: 'ggplot2' Pattern Geoms.
891 <https://CRAN.R-project.org/package=ggpattern>
892
- 893 Felix, M. A. (2008, Nov 13). RNA interference in nematodes and the chance that favored
894 Sydney Brenner. *J Biol*, 7(9), 34. <https://doi.org/10.1186/jbiol97>
895
- 896 Felix, M. A., Ashe, A., Piffaretti, J., Wu, G., Nuez, I., Belicard, T., Jiang, Y., Zhao, G., Franz, C.
897 J., Goldstein, L. D., Sanroman, M., Miska, E. A., & Wang, D. (2011, Jan 25). Natural and
898 experimental infection of Caenorhabditis nematodes by novel viruses related to
899 nodaviruses. *PLoS Biol*, 9(1), e1000586. <https://doi.org/10.1371/journal.pbio.1000586>
900
- 901 Fire, A., Xu, S., Montgomery, M. K., Kostas, S. A., Driver, S. E., & Mello, C. C. (1998, Feb 19).
902 Potent and specific genetic interference by double-stranded RNA in Caenorhabditis
903 elegans. *Nature*, 391(6669), 806-811. <https://doi.org/10.1038/35888>
904
- 905 Frezal, L., Demoinet, E., Braendle, C., Miska, E., & Felix, M. A. (2018, Aug 20). Natural Genetic
906 Variation in a Multigenerational Phenotype in *C. elegans*. *Curr Biol*, 28(16), 2588-2596
907 e2588. <https://doi.org/10.1016/j.cub.2018.05.091>
908
- 909 Gaertner, B. E., & Phillips, P. C. (2010, Dec). Caenorhabditis elegans as a platform for
910 molecular quantitative genetics and the systems biology of natural variation. *Genet Res*
911 *(Camb)*, 92(5-6), 331-348. <https://doi.org/10.1017/S0016672310000601>
912
- 913 Gao, C.-H. (2021). ggVennDiagram: A 'ggplot2' Implement of Venn Diagram. [https://CRAN.R-](https://CRAN.R-project.org/package=ggVennDiagram)
914 [project.org/package=ggVennDiagram](https://CRAN.R-project.org/package=ggVennDiagram)
915
- 916 Ghosh, R., Bloom, J. S., Mohammadi, A., Schumer, M. E., Andolfatto, P., Ryu, W., & Kruglyak,
917 L. (2015, Aug). Genetics of Intraspecies Variation in Avoidance Behavior Induced by a
918 Thermal Stimulus in Caenorhabditis elegans. *Genetics*, 200(4), 1327-1339.
919 <https://doi.org/10.1534/genetics.115.178491>
920
- 921 Grishok, A., Pasquinelli, A. E., Conte, D., Li, N., Parrish, S., Ha, I., Baillie, D. L., Fire, A.,
922 Ruvkun, G., & Mello, C. C. (2001, Jul 13). Genes and mechanisms related to RNA
923 interference regulate expression of the small temporal RNAs that control *C. elegans*
924 developmental timing. *Cell*, 106(1), 23-34. [https://doi.org/10.1016/s0092-8674\(01\)00431-](https://doi.org/10.1016/s0092-8674(01)00431-7)
925 [7](https://doi.org/10.1016/s0092-8674(01)00431-7)
926
- 927 Hahnel, S. R., Zdraljevic, S., Rodriguez, B. C., Zhao, Y., McGrath, P. T., & Andersen, E. C.
928 (2018, Oct). Extreme allelic heterogeneity at a Caenorhabditis elegans beta-tubulin locus
929 explains natural resistance to benzimidazoles. *PLoS Pathog*, 14(10), e1007226.
930 <https://doi.org/10.1371/journal.ppat.1007226>
931
- 932 Harris, T. W., Arnaboldi, V., Cain, S., Chan, J., Chen, W. J., Cho, J., Davis, P., Gao, S., Grove,
933 C. A., Kishore, R., Lee, R. Y. N., Muller, H. M., Nakamura, C., Nuin, P., Paulini, M.,
934 Raciti, D., Rodgers, F. H., Russell, M., Schindelman, G., Auken, K. V., Wang, Q.,
935 Williams, G., Wright, A. J., Yook, K., Howe, K. L., Schedl, T., Stein, L., & Sternberg, P.
936 W. (2020, Jan 8). WormBase: a modern Model Organism Information Resource. *Nucleic*
937 *Acids Res*, 48(D1), D762-D767. <https://doi.org/10.1093/nar/gkz920>

- 938
939 He, F. (2011, 2011/03/20). Total RNA Extraction from *C. elegans*. *Bio-protocol*, 1(6), e47.
940 <https://doi.org/10.21769/BioProtoc.47>
941
942 Kamath, R. S., & Ahringer, J. (2003, Aug). Genome-wide RNAi screening in *Caenorhabditis*
943 *elegans*. *Methods*, 30(4), 313-321. [https://doi.org/10.1016/s1046-2023\(03\)00050-1](https://doi.org/10.1016/s1046-2023(03)00050-1)
944
945 Kamath, R. S., Martinez-Campos, M., Zipperlen, P., Fraser, A. G., & Ahringer, J. (2001).
946 Effectiveness of specific RNA-mediated interference through ingested double-stranded
947 RNA in *Caenorhabditis elegans*. *Genome Biol*, 2(1), RESEARCH0002.
948 <https://doi.org/10.1186/gb-2000-2-1-research0002>
949
950 Larsson, J. (2021). eulerr: Area-Proportional Euler and Venn Diagrams with Ellipses.
951 <https://CRAN.R-project.org/package=eulerr>
952
953 Lee, D., Zdraljevic, S., Stevens, L., Wang, Y., Tanny, R. E., Crombie, T. A., Cook, D. E.,
954 Webster, A. K., Chirakar, R., Baugh, L. R., Sterken, M. G., Braendle, C., Felix, M. A.,
955 Rockman, M. V., & Andersen, E. C. (2021, Jun). Balancing selection maintains hyper-
956 divergent haplotypes in *Caenorhabditis elegans*. *Nat Ecol Evol*, 5(6), 794-807.
957 <https://doi.org/10.1038/s41559-021-01435-x>
958
959 Lee, S. H., Wong, R. R., Chin, C. Y., Lim, T. Y., Eng, S. A., Kong, C., Ijap, N. A., Lau, M. S.,
960 Lim, M. P., Gan, Y. H., He, F. L., Tan, M. W., & Nathan, S. (2013, Sep 10). *Burkholderia*
961 *pseudomallei* suppresses *Caenorhabditis elegans* immunity by specific degradation of a
962 GATA transcription factor. *Proc Natl Acad Sci U S A*, 110(37), 15067-15072.
963 <https://doi.org/10.1073/pnas.1311725110>
964
965 Li, H.-D. (2018). GTFtools: a Python package for analyzing various modes of gene models.
966 *bioRxiv*, 263517. <https://doi.org/10.1101/263517>
967
968 Love, M. I., Huber, W., & Anders, S. (2014). Moderated estimation of fold change and
969 dispersion for RNA-seq data with DESeq2. *Genome Biol*, 15(12), 550.
970 <https://doi.org/10.1186/s13059-014-0550-8>
971
972 McGrath, P. T., Rockman, M. V., Zimmer, M., Jang, H., Macosko, E. Z., Kruglyak, L., &
973 Bargmann, C. I. (2009, Mar 12). Quantitative mapping of a digenic behavioral trait
974 implicates globin variation in *C. elegans* sensory behaviors. *Neuron*, 61(5), 692-699.
975 <https://doi.org/10.1016/j.neuron.2009.02.012>
976
977 Na, H., Zdraljevic, S., Tanny, R. E., Walhout, A. J. M., & Andersen, E. C. (2020, Aug). Natural
978 variation in a glucuronosyltransferase modulates propionate sensitivity in a *C. elegans*
979 propionic acidemia model. *PLoS Genet*, 16(8), e1008984.
980 <https://doi.org/10.1371/journal.pgen.1008984>
981
982 Neuwirth, E. (2022). RColorBrewer: ColorBrewer Palettes. [https://CRAN.R-](https://CRAN.R-project.org/package=RColorBrewer)
983 [project.org/package=RColorBrewer](https://CRAN.R-project.org/package=RColorBrewer)
984
985 Paaby, A. B., White, A. G., Riccardi, D. D., Gunsalus, K. C., Piano, F., & Rockman, M. V. (2015,
986 Aug 22). Wild worm embryogenesis harbors ubiquitous polygenic modifier variation.
987 *Elife*, 4. <https://doi.org/10.7554/eLife.09178>
988

- 989 Patro, R., Duggal, G., Love, M. I., Irizarry, R. A., & Kingsford, C. (2017, Apr). Salmon provides
990 fast and bias-aware quantification of transcript expression. *Nat Methods*, 14(4), 417-419.
991 <https://doi.org/10.1038/nmeth.4197>
992
- 993 Pedersen, B. S., & Quinlan, A. R. (2018, Mar 1). Mosdepth: quick coverage calculation for
994 genomes and exomes. *Bioinformatics*, 34(5), 867-868.
995 <https://doi.org/10.1093/bioinformatics/btx699>
996
- 997 Pertea, G., & Pertea, M. (2020). GFF Utilities: GffRead and GffCompare. *F1000Res*, 9.
998 <https://doi.org/10.12688/f1000research.23297.2>
999
- 1000 Pollard, D. A., & Rockman, M. V. (2013, Jun 21). Resistance to germline RNA interference in a
1001 *Caenorhabditis elegans* wild isolate exhibits complexity and nonadditivity. *G3 (Bethesda,*
1002 *Md.)*, 3(6), 941-947. <https://doi.org/10.1534/g3.113.005785>
1003
- 1004 R Core Team. (2021). *R: A language and environment for statistical computing*. R Foundation
1005 for Statistical Computing. <https://www.R-project.org/>
1006
- 1007 Rockman, M. V., Skrovaneck, S. S., & Kruglyak, L. (2010, Oct 15). Selection at linked sites
1008 shapes heritable phenotypic variation in *C. elegans*. *Science*, 330(6002), 372-376.
1009 <https://doi.org/10.1126/science.1194208>
1010
- 1011 Saber, S., Snyder, M., Rajaei, M., & Baer, C. F. (2022, May 6). Mutation, selection, and the
1012 prevalence of the *Caenorhabditis elegans* heat-sensitive mortal germline phenotype. *G3*
1013 *(Bethesda, Md.)*, 12(5). <https://doi.org/10.1093/g3journal/jkac063>
1014
- 1015 Sijen, T., Fleenor, J., Simmer, F., Thijssen, K. L., Parrish, S., Timmons, L., Plasterk, R. H., &
1016 Fire, A. (2001, Nov 16). On the role of RNA amplification in dsRNA-triggered gene
1017 silencing. *Cell*, 107(4), 465-476. [https://doi.org/10.1016/s0092-8674\(01\)00576-1](https://doi.org/10.1016/s0092-8674(01)00576-1)
1018
- 1019 Sonesson, C., Love, M. I., & Robinson, M. D. (2015). Differential analyses for RNA-seq:
1020 transcript-level estimates improve gene-level inferences. *F1000Res*, 4, 1521.
1021 <https://doi.org/10.12688/f1000research.7563.2>
1022
- 1023 Stephens, M. (2017, Apr 1). False discovery rates: a new deal. *Biostatistics*, 18(2), 275-294.
1024 <https://doi.org/10.1093/biostatistics/kxw041>
1025
- 1026 Stiernagle, T. (2006, Feb 11). Maintenance of *C. elegans*. *WormBook*, 1-11.
1027 <https://doi.org/10.1895/wormbook.1.101.1>
1028
- 1029 Tijsterman, M., Okihara, K. L., Thijssen, K., & Plasterk, R. H. (2002, Sep 3). PPW-1, a
1030 PAZ/PIWI protein required for efficient germline RNAi, is defective in a natural isolate of
1031 *C. elegans*. *Curr Biol*, 12(17), 1535-1540. [https://doi.org/10.1016/s0960-9822\(02\)01110-](https://doi.org/10.1016/s0960-9822(02)01110-7)
1032 [7](https://doi.org/10.1016/s0960-9822(02)01110-7)
1033
- 1034 Vinuela, A., Snoek, L. B., Riksen, J. A., & Kammenga, J. E. (2010, Jul). Genome-wide gene
1035 expression regulation as a function of genotype and age in *C. elegans*. *Genome Res*,
1036 20(7), 929-937. <https://doi.org/10.1101/gr.102160.109>
1037
- 1038 Webster, A. K., Hung, A., Moore, B. T., Guzman, R., Jordan, J. M., Kaplan, R. E. W., Hibshman,
1039 J. D., Tanny, R. E., Cook, D. E., Andersen, E., & Baugh, L. R. (2019). Population

- 1040 Selection and Sequencing of *Caenorhabditis elegans* Wild Isolates Identifies a Region
1041 on Chromosome III Affecting Starvation Resistance. *G3 (Bethesda, Md.)*, 9(10), 3477-
1042 3488. Retrieved 2019/10//, from <http://europepmc.org/abstract/MED/31444297>
1043 <https://doi.org/10.1534/g3.119.400617>
1044 <https://europepmc.org/articles/PMC6778785>
1045 <https://europepmc.org/articles/PMC6778785?pdf=render>
1046
1047 Wickham, H. (2016). *ggplot2: Elegant Graphics for Data Analysis*. Springer-Verlag New York.
1048 <https://ggplot2.tidyverse.org>
1049
1050 Wilke, C. O. (2020). cowplot: Streamlined Plot Theme and Plot Annotations for 'ggplot2'.
1051 <https://CRAN.R-project.org/package=cowplot>
1052
1053 Wilson, R. C., & Doudna, J. A. (2013). Molecular mechanisms of RNA interference. *Annu Rev*
1054 *Biophys*, 42, 217-239. <https://doi.org/10.1146/annurev-biophys-083012-130404>
1055
1056 Zamanian, M., Cook, D. E., Zdraljevic, S., Brady, S. C., Lee, D., Lee, J., & Andersen, E. C.
1057 (2018, Mar). Discovery of genomic intervals that underlie nematode responses to
1058 benzimidazoles. *PLoS Negl Trop Dis*, 12(3), e0006368.
1059 <https://doi.org/10.1371/journal.pntd.0006368>
1060
1061 Zan, Y., Shen, X., Forsberg, S. K., & Carlborg, O. (2016, Aug 9). Genetic Regulation of
1062 Transcriptional Variation in Natural *Arabidopsis thaliana* Accessions. *G3 (Bethesda,*
1063 *Md.)*, 6(8), 2319-2328. <https://doi.org/10.1534/g3.116.030874>
1064
1065 Zdraljevic, S., Fox, B. W., Strand, C., Panda, O., Tenjo, F. J., Brady, S. C., Crombie, T. A.,
1066 Doench, J. G., Schroeder, F. C., & Andersen, E. C. (2019, Apr 8). Natural variation in *C.*
1067 *elegans* arsenic toxicity is explained by differences in branched chain amino acid
1068 metabolism. *Elife*, 8. <https://doi.org/10.7554/eLife.40260>
1069
1070 Zdraljevic, S., Strand, C., Seidel, H. S., Cook, D. E., Doench, J. G., & Andersen, E. C. (2017,
1071 Jul). Natural variation in a single amino acid substitution underlies physiological
1072 responses to topoisomerase II poisons. *PLoS Genet*, 13(7), e1006891.
1073 <https://doi.org/10.1371/journal.pgen.1006891>
1074
1075 Zhang, G., Roberto, N. M., Lee, D., Hahnel, S. R., & Andersen, E. C. (2022, Jun 16). The
1076 impact of species-wide gene expression variation on *Caenorhabditis elegans* complex
1077 traits. *Nat Commun*, 13(1), 3462. <https://doi.org/10.1038/s41467-022-31208-4>
1078

1079